Supplementary Information

Synthetic β-cells for fusion-mediated dynamic insulin secretion

Zhaowei Chen[1,2,4], Jinqiang Wang[1,2,4], Wujin Sun[1,2], Edikan Archibong[1], Anna R. Kahkoska[3], Xudong Zhang[1,2], Yue Lu[1,2], Frances S. Ligler[1], John B. Buse[3] and Zhen Gu[1,2,3,*]

[1]Joint Department of Biomedical Engineering, University of North Carolina at Chapel Hill and North Carolina State University, Raleigh, NC 27695, USA

[2]Division of Pharmacoengineering and Molecular Pharmaceutics and Center for Nanotechnology in Drug Delivery, Eshelman School of Pharmacy, University of North Carolina at Chapel Hill, Chapel Hill, NC 27599, USA

[3]Department of Medicine, University of North Carolina School of Medicine, Chapel Hill, NC 27599, USA

[4]These authors contributed equally to this work.

*Corresponding author. Email: zgu@email.unc.edu

Supplementary Results

Supplementary Figures:

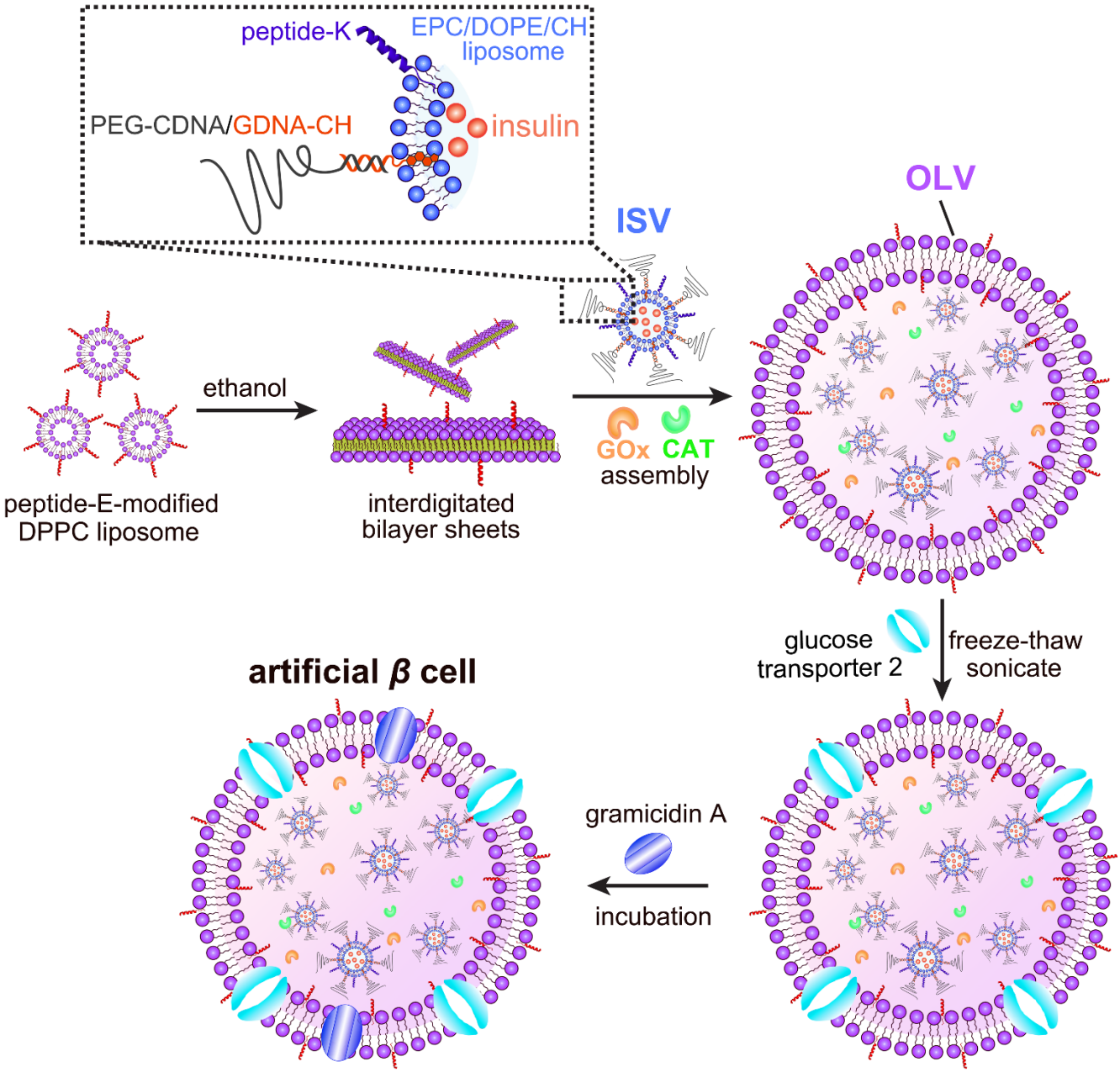

Supplementary Figure 1| Schematic illustration of the design and synthesis of the artificial β-cell. GOx, CAT, ISV and OLV are abbreviations for glucose oxidase, catalase, inner small vesicle and outer large vesicle, respectively.

Nature Chemical Biology: doi:10.1038/nchembio.2511

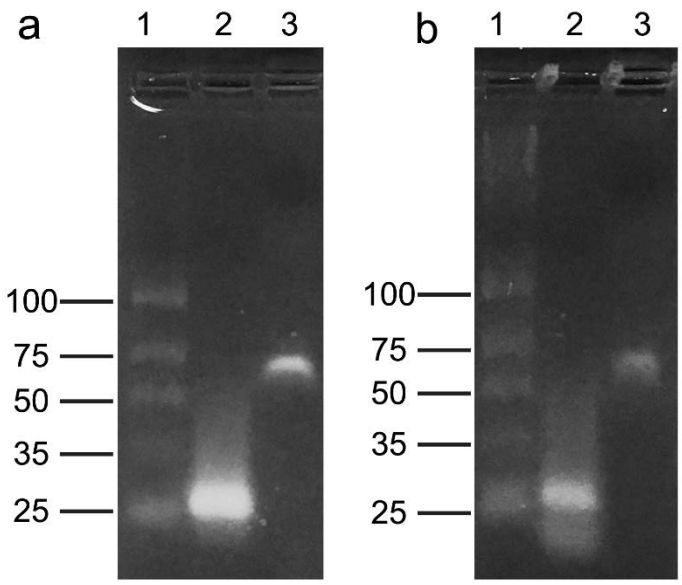

Supplementary Figure 2| a, Agarose (2%) electrophoresis of DNA ladder (lane 1), cytosine-rich DNA (CDNA, lane 2) and PEG_{5000} conjugated CDNA (lane 3); **b,** Agarose (2%) electrophoresis of DNA-ladder (lane 1), control DNA1 (lane 2) and PEG_{5000} conjugated DNA1 (lane 3).

Nature Chemical Biology: doi:10.1038/nchembio.2511

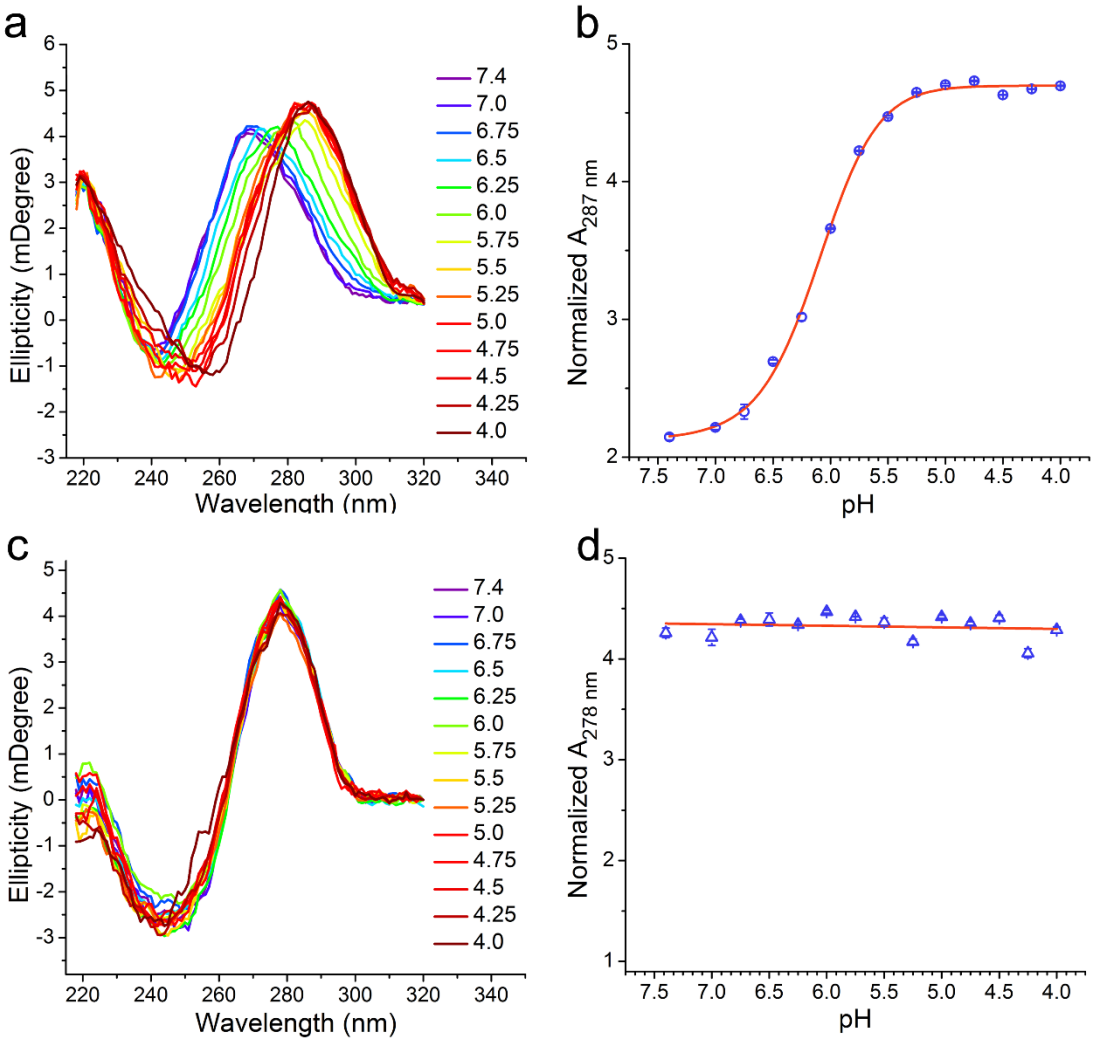

Supplementary Figure 3| CD spectra of PEG-CDNA/GDNA-CH (**a**) and PEG-DNA1/DNA2-CH (**c**) that illustrate DNA conformational changes at different pH's. **b,** the CD intensity of the characteristic band of tetraplex DNA (summation of i-motif and G-quadruplex) around 287 nm versus different pH values while (**d**) shows the CD intensity of the characteristic band of duplex DNA at 278 nm versus pH values. From the results, it can be concluded that PEG-CDNA/GDNA-CH dehybridized and formed tetraplexes below pH 5.5 while the control PEG-DNA1/DNA2-CH showed no dissociation during the studied pH range. Data points represent mean ± SD (three independent experiments per group; n=3).

Nature Chemical Biology: doi:10.1038/nchembio.2511

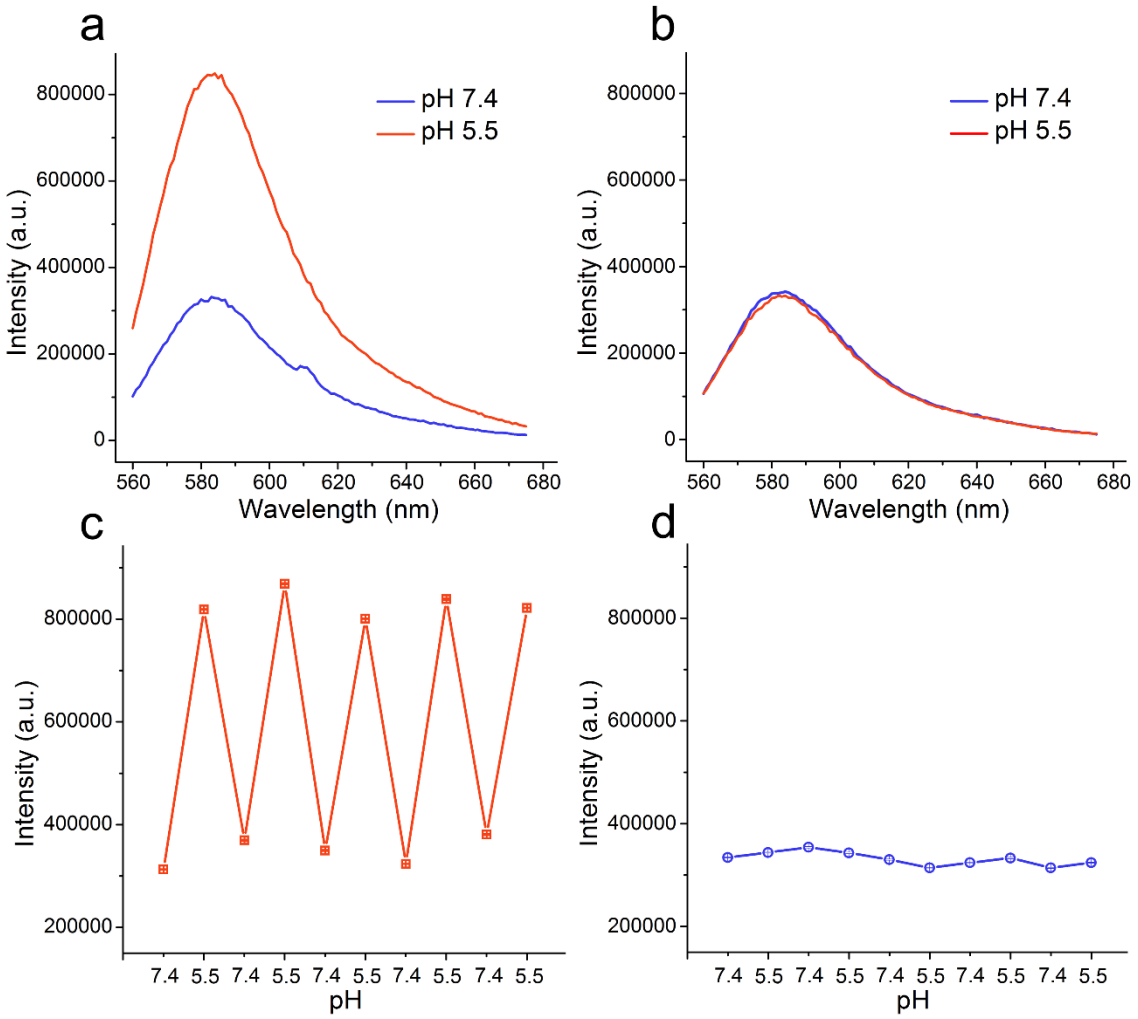

Supplementary Figure 4| Reversible, pH-controlled attachment/detachment of PEG shield on the ISV surface studied using a fluorescent resonance energy transfer (FRET) assay. Fluorescent spectra of (**a**) PEG_{5000}-conjuagted C-rich DNA (labeled with tetramethylrhodamine, DNA-donor)/cholesterol-ended G-rich DNA (labeled with IAbRQ, DNA-acceptor)-inserted ISVs and (**b**) PEG_{5000}-DNA1 (labeled with DNA-donor)/DNA2 (labeled with DNA acceptor)-cholesterol-inserted ISVs at pH 7.4 and pH 5.5 with excitation at 555 nm. See supplementary Table 1 for DNA sequence details. (**c**) and (**d**), respectively showed the fluorescence intensity of DNA-donor in (a) and (b) at different cycles of switching pH at 7.4 and 5.5. The fluorescence intensity at each cycle was measured 20 min after switching the pH. Data points represent mean ± SD (three independent experiments per group; n=3).

Nature Chemical Biology: doi:10.1038/nchembio.2511

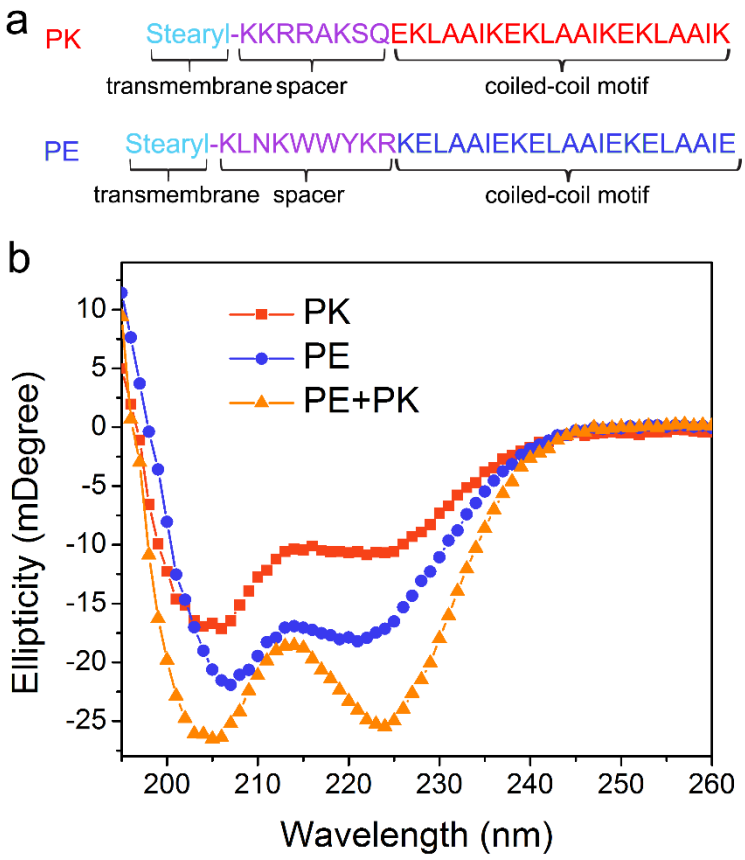

Supplementary Figure 5| a, Sequences of peptide-K and peptide-E with three components-a transmembrane domain, a spacer and a recognition motif, mimicking the membrane fusion SNARE proteins (SNARE = soluble NSF attachment protein receptor). The sequences were designed by modifying previously reported peptides.[30, 31] **b,** CD spectra of peptide-E, peptide-K, and peptide-E/peptide-K. From the CD spectra it can be seen that peptide-K show a substantial α-helical content ($[\theta]_{220nm}/[\theta]_{208nm}$ is ~0.71), whereas peptide-E adopts a predominantly random coil structure. After mixing, the α-helix content increases as the ratio of $[\theta]_{220nm}/[\theta]_{208nm}$ is around 1, confirming the formation of coiled-coil structures between peptide-E and peptide-K.

Nature Chemical Biology: doi:10.1038/nchembio.2511

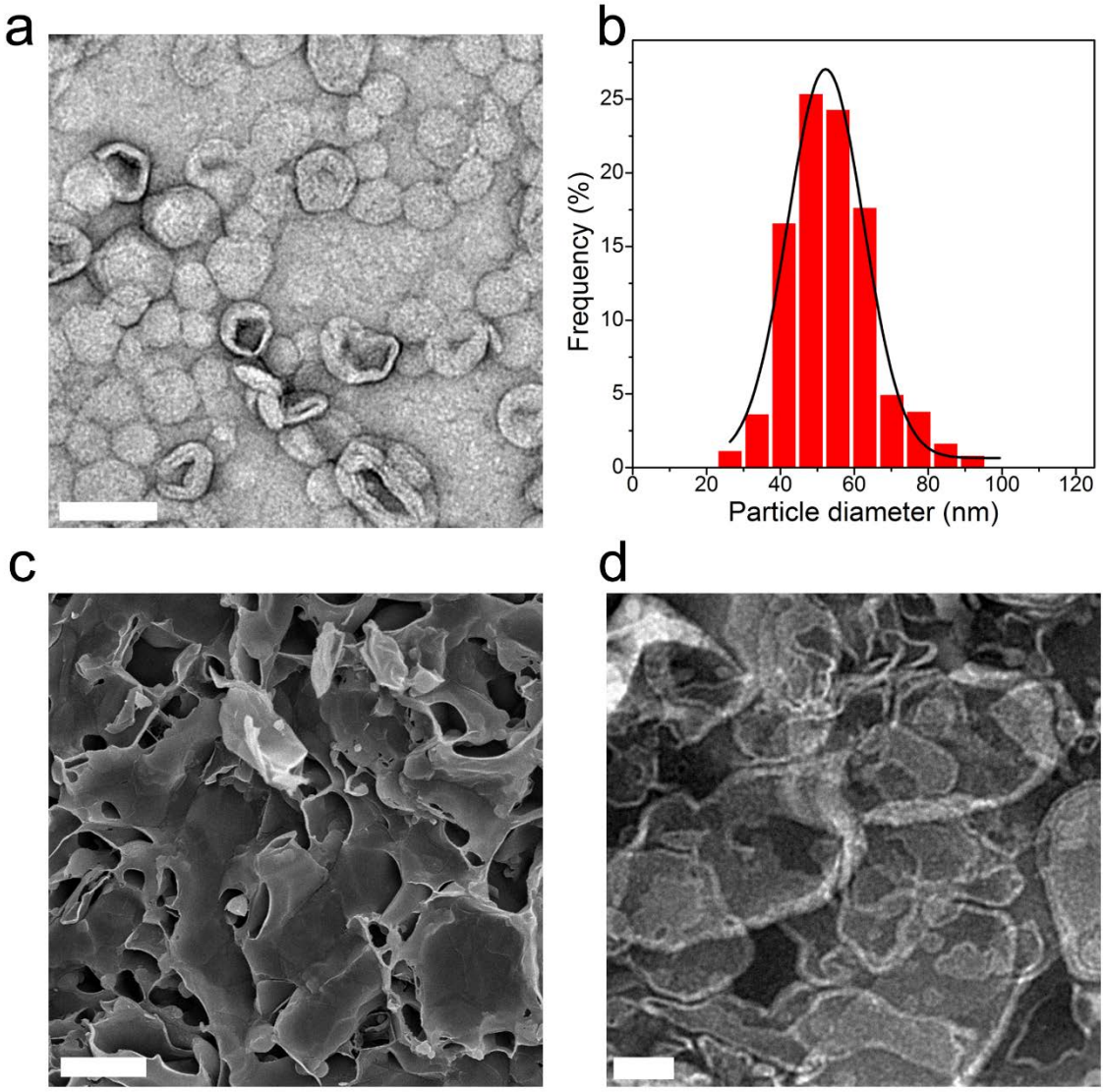

Supplementary Figure 6| a, Transmission electron microscopy image (TEM) of the DPPC liposomes (scale bar, 100 nm); **b,** Size distribution histogram of the liposomes shown in panel **a**; cryogenic scanning electron microscopy (**c**) and TEM (**d**) of the interdigitated bilayer sheets made from the DPPC liposomes (**c** scale bar, 2 μm; **d** scale bar, 100 nm).

Nature Chemical Biology: doi:10.1038/nchembio.2511

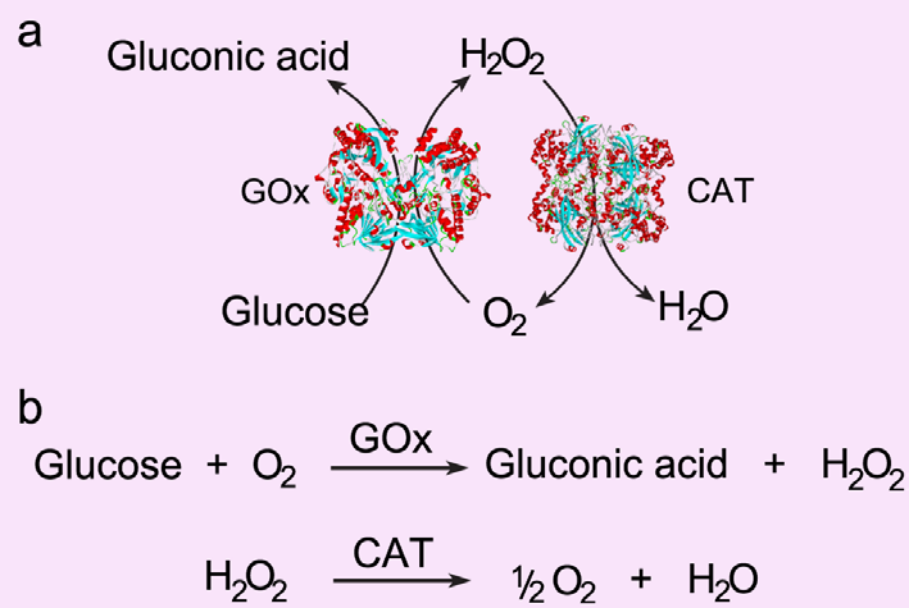

Supplementary Figure 7| (**a**) Schematic illustration and (**b**) reaction equations of the enzymatic reactions involving glucose oxidation catalyzed by glucose oxidase (GOx) and hydrogen peroxide breakdown by catalase (CAT). The decomposition of the undesired hydrogen peroxide can regenerate oxygen to facilitate glucose oxidation.

Nature Chemical Biology: doi:10.1038/nchembio.2511

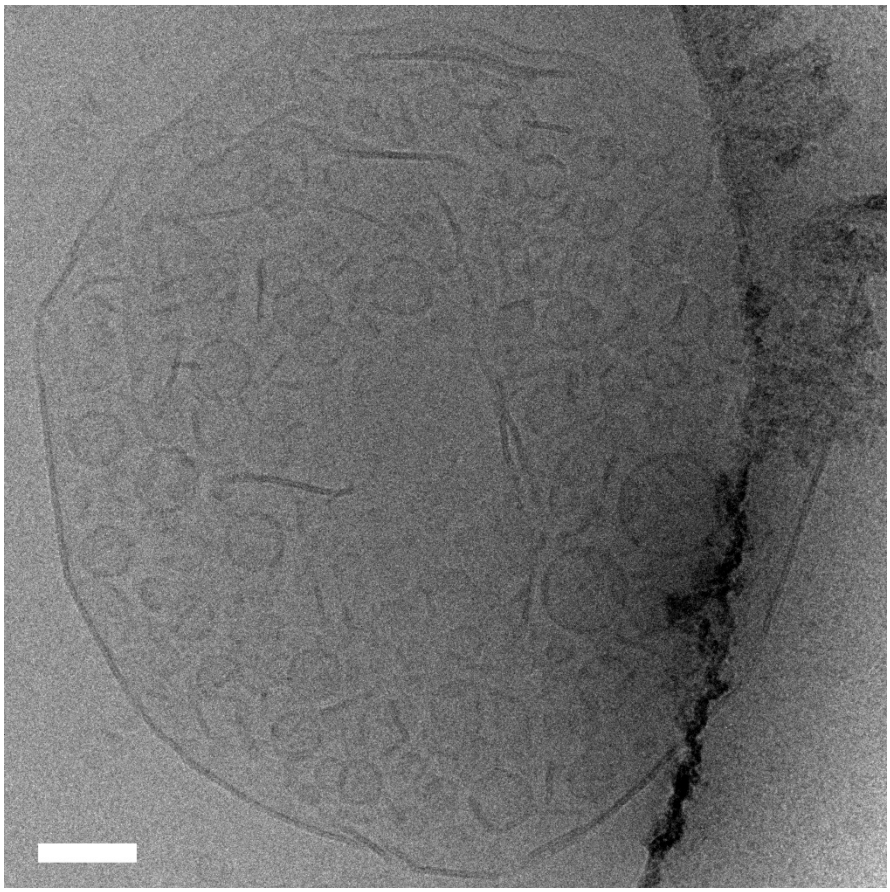

Supplementary Figure 8| A representative cryogenic transmission electron microscopy (cryoTEM) image of the final vesicles-in-vesicle superstructures. Scale bar: 100 nm.

Nature Chemical Biology: doi:10.1038/nchembio.2511

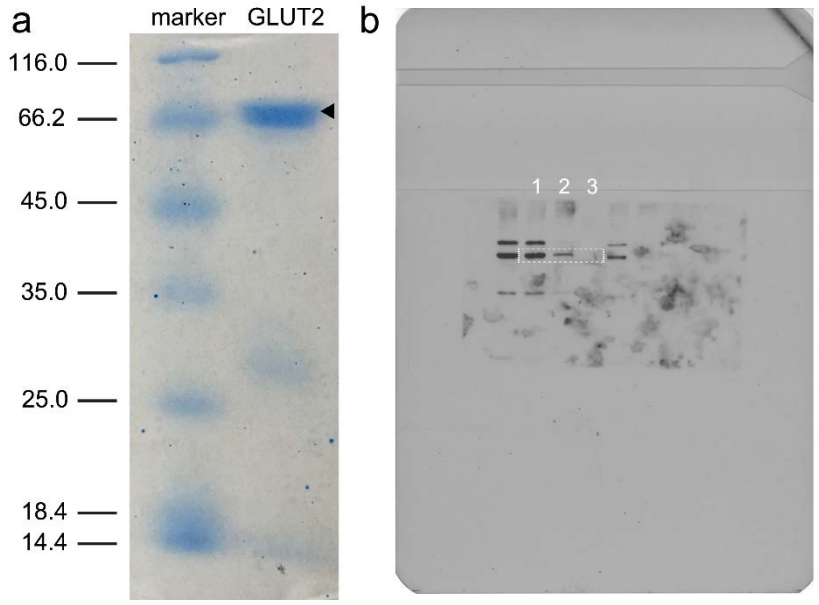

Supplementary Figure 9| (a) SDS-PAGE analysis of the purified glucose transporter 2 (GLUT2). (b) Uncropped western blots for Figure 1f. Lanes used for Figure 1f are indicated by a rectangle, where Lane 1, 2 and 3 respectively represent the blots of GLUT2, liposomal superstructures inserted with GLUT2, and pure liposomal superstructures. The lanes on the left side of lane 1 and right side of lane 3 are GLUT2 isolated from different batches of bacteria.

Nature Chemical Biology: doi:10.1038/nchembio.2511

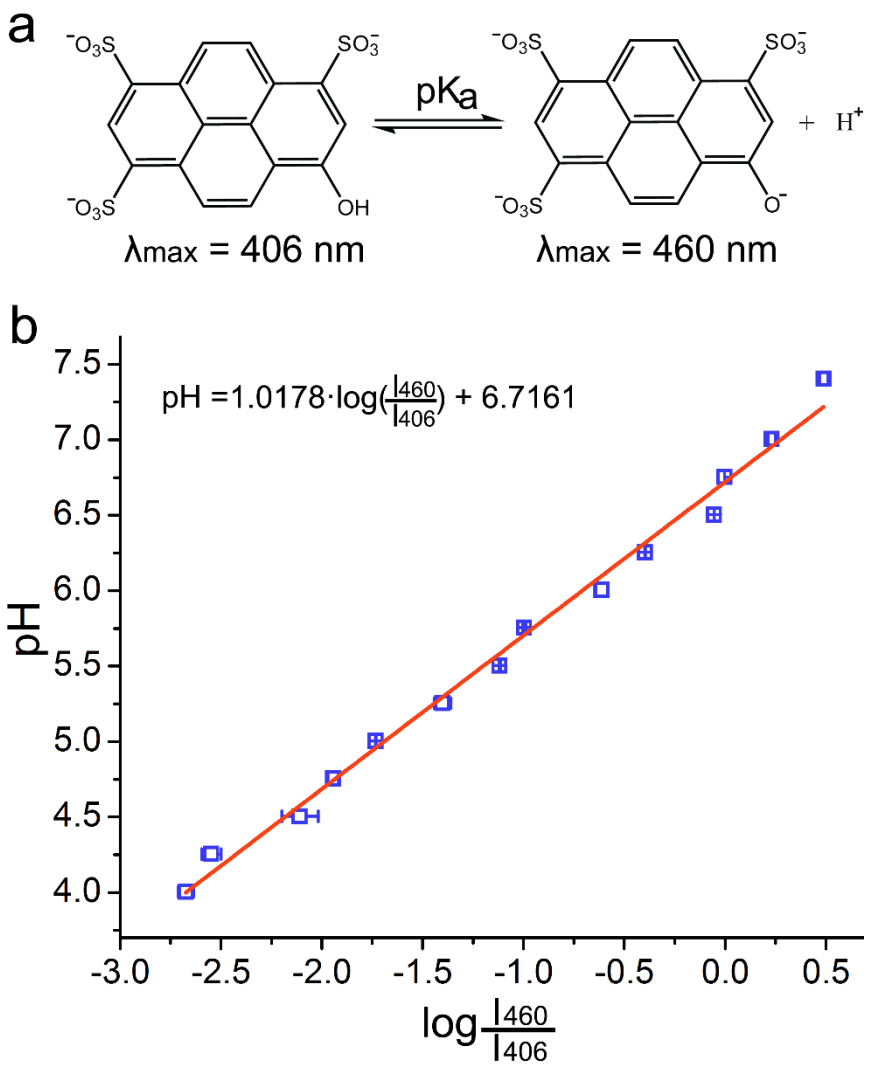

Supplementary Figure 10| a, Unionized and ionized forms of HPTS (pK_a = 7.2). **b,** pH titrations of the relative fluorescence intensities of HPTS excited at 406 nm and 460 nm (HEPES buffer, 5 mM, 100 mM NaCl). The fluorescence intensities of HPTS at 514 nm excited by 406 (I_{406}) and 460 (I_{460}) nm were strongly dependent on the degree of ionization of the 8-hydroxyl group and hence on the medium pH. Data points represent mean ± SD (three independent experiments per group; n=3).

Nature Chemical Biology: doi:10.1038/nchembio.2511

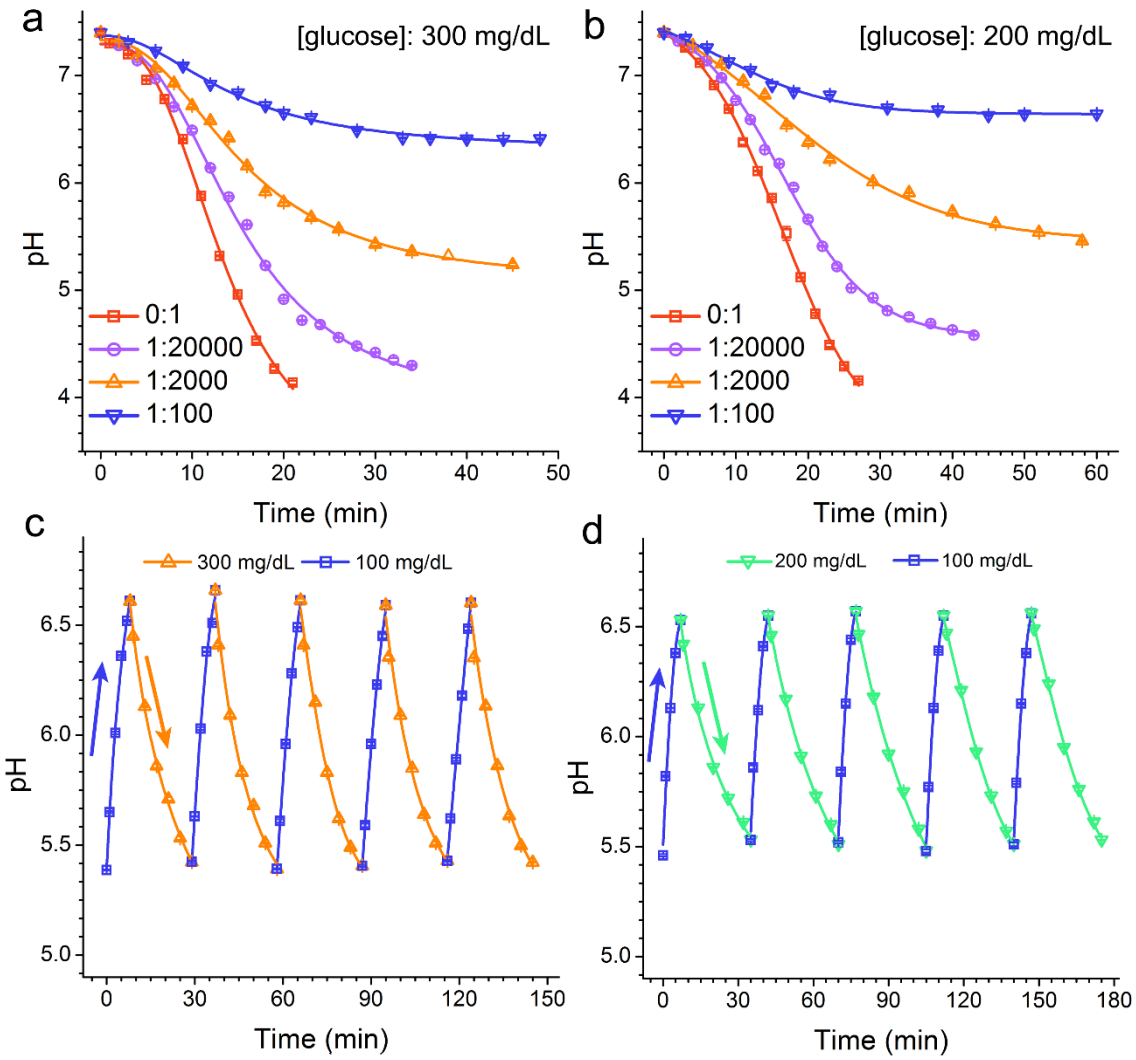

Supplementary Figure 11| pH variation inside AβCs at modest glucose concentrations with different gramicidin insertion in (**a**) 300 mg/dL and (**b**) 200 mg/dL glucose solutions. The ratio in the figure label indicates the ratio of gramicidin-to- dipalmitoylphosphatidylcholine lipid. **c, d,** Reversible pH variation as a result of alternatively switching environmental glucose concentrations. Data points represent mean ± SD (three independent experiments per group; n=3).

Nature Chemical Biology: doi:10.1038/nchembio.2511

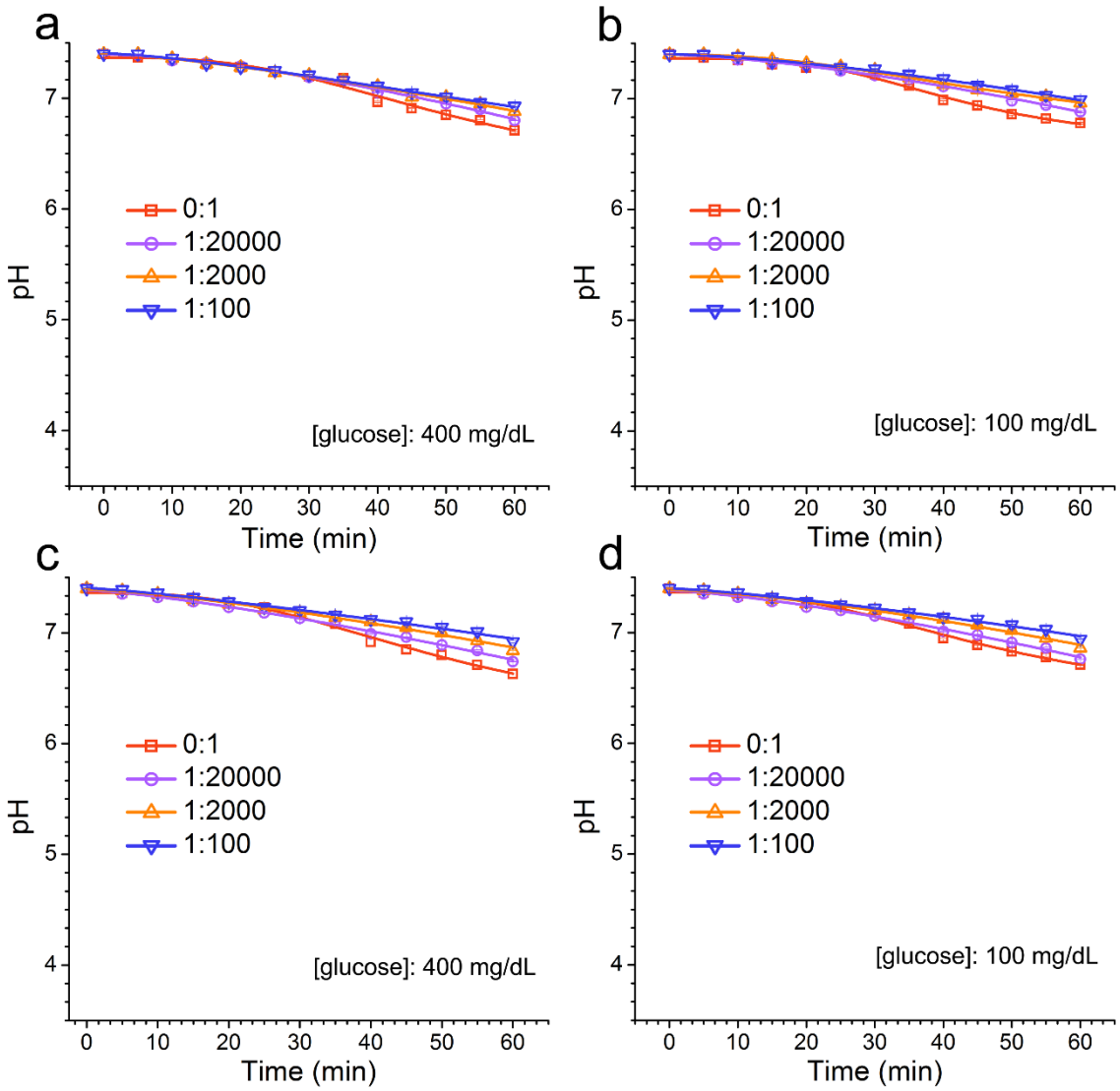

Supplementary Figure 12| pH changes inside control AβCs with no glucose transporter 2 reconstitution in (**a**) 400 md/dL and (**b**) 100 mg/dL glucose solutions, and glucose transporter 2 inhibitor-Cytochalasin B pre-treated AβCs in (**c**) 400 md/dL and (**d**) 100 mg/dL glucose solutions. The ratios in the figure represent the molar ratio of the added GA-to-lipid of the outer large liposomal vesicles. In all the control groups, no significant pH variation was observed compared to their counterparts in the experimental group over the same time. The slower decrease in pH might be induced by the passive diffusion of glucose into the control AβCs. These results indicated that glucose transporter 2 was responsible for the uptake of glucose into AβC, ensued which glucose oxidation induced the pH variation. Data points represent mean ± SD (three independent experiments per group; n=3).

Nature Chemical Biology: doi:10.1038/nchembio.2511

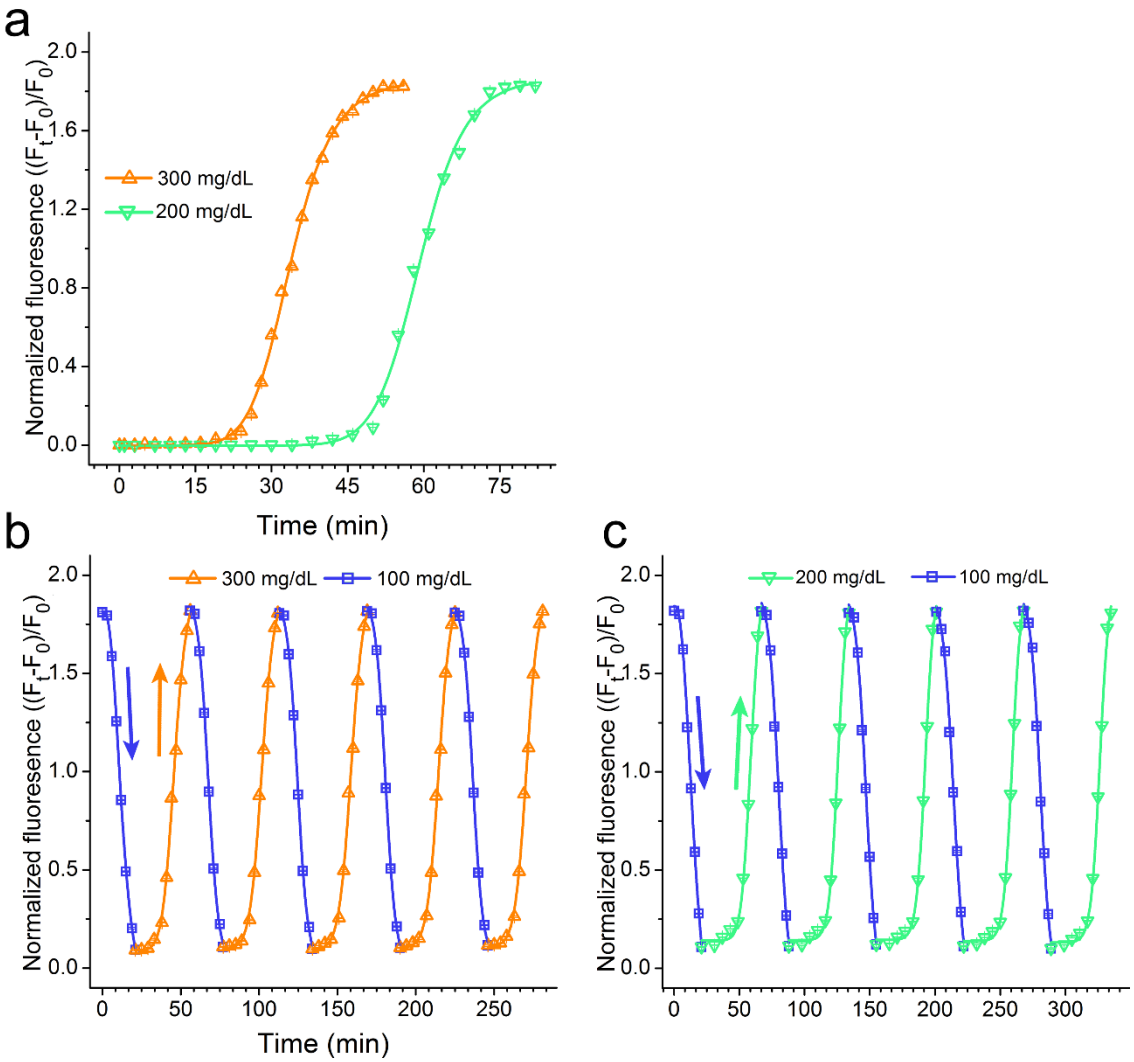

Supplementary Figure 13| a, FRET assay to study the dehybridization of the pH-sensitive DNA duplex which bridges the PEG shield and the ISV surface, accompanying the glucose metabolism by AβCs in 300 mg/mL and 200 mg/mL glucose solutions. F_0 and F_t represent the fluorescence intensity measured before and at time t after addition into glucose solutions. **b** and **c**, Reversible quenching and recovery of the fluorescence of DNA-donor to demonstrate the reversible attachment and detachment of the PEG shield at high and low glucose solutions. Data points represent mean ± SD (three independent experiments per group; n=3).

Nature Chemical Biology: doi:10.1038/nchembio.2511

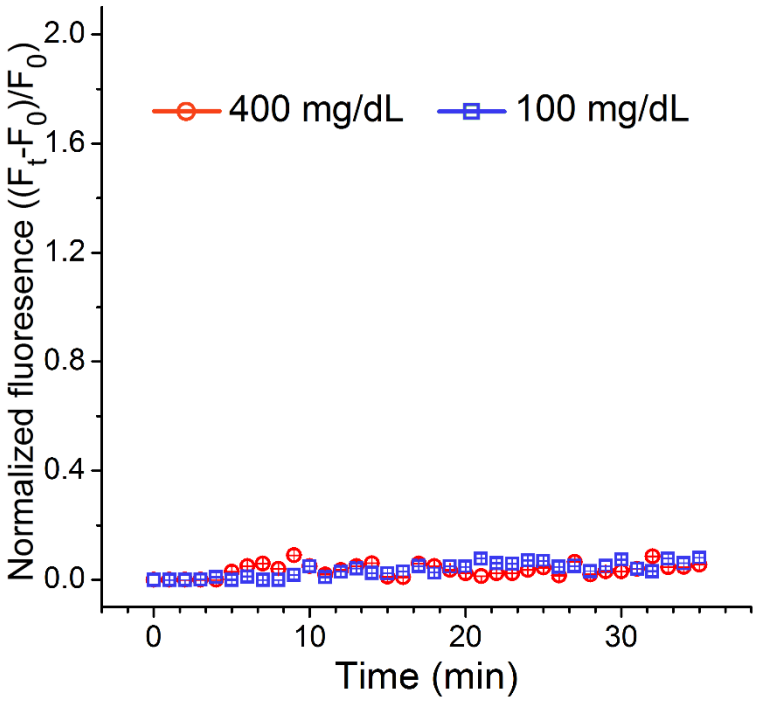

Supplementary Figure 14| FRET assay to study the dehybridization of the non-pH-sensitive DNA duplex which bridges the PEG shield and the ISV surface, accompanying the glucose metabolism by AβCs in 400 mg/mL and 100 mg/mL glucose solutions. F_0 and F_t represent the fluorescence intensity measured before and at time t after addition into glucose solutions. The results indicated that no disassociation of the control duplex DNA occurred at either high or low glucose levels due to the lack of pH-sensitive properties. The fluorophore and quencher modification information was shown in the Supplementary Table S1. Data points represent mean ± SD (three independent experiments per group; n=3).

Nature Chemical Biology: doi:10.1038/nchembio.2511

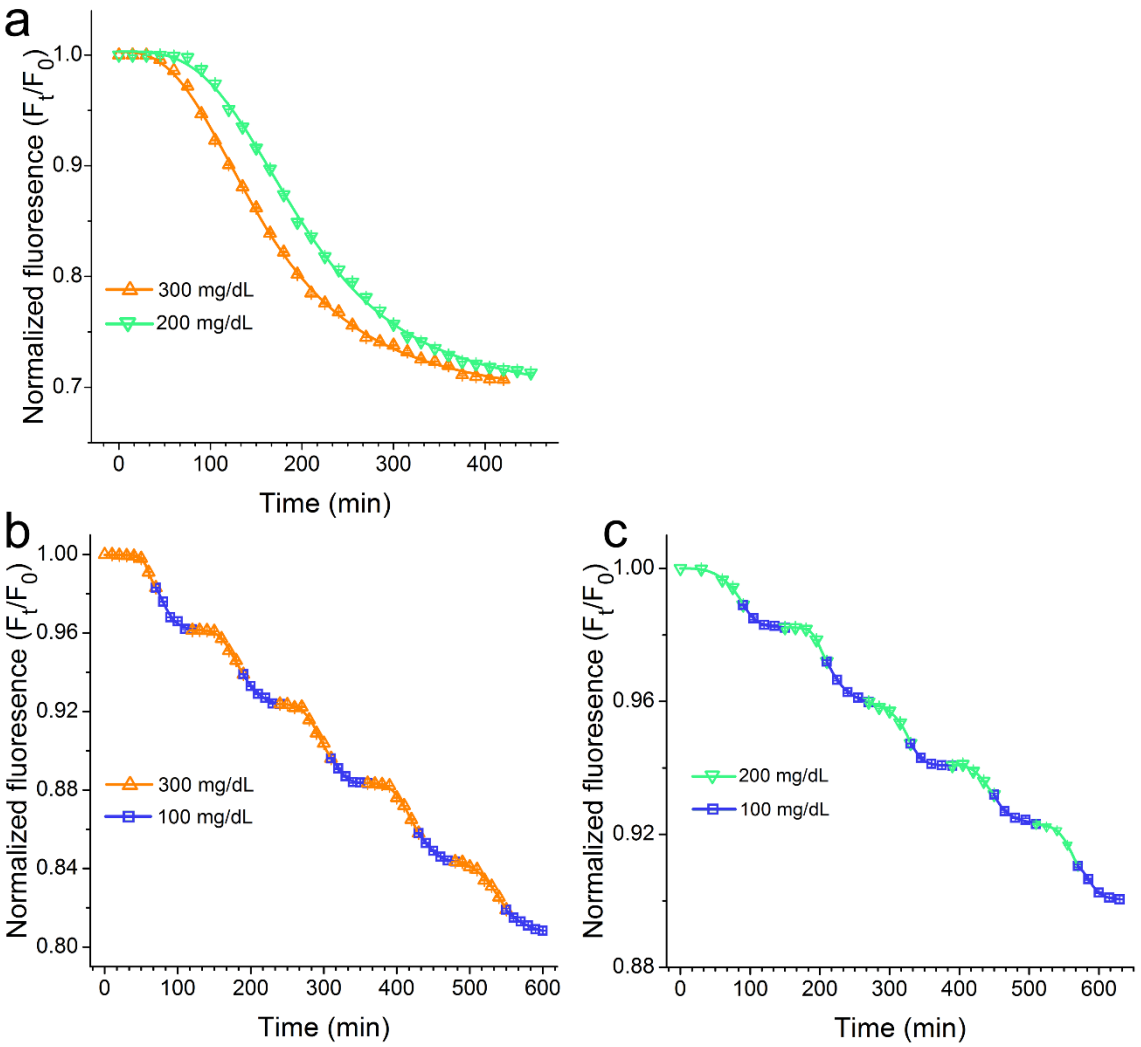

Supplementary Figure 15| a, FRET assay to study the interactions of peptide-E and peptide-K at modest hyperglycemic concentrations. F_0 and F_t represent the fluorescence intensity measured before and at time t after addition into glucose solutions. **b** and **c**, Step decrease in fluorescence intensity of peptide-donor by switching the glucose concentrations. Data points represent mean ± SD (three independent experiments per group; n=3).

Nature Chemical Biology: doi:10.1038/nchembio.2511

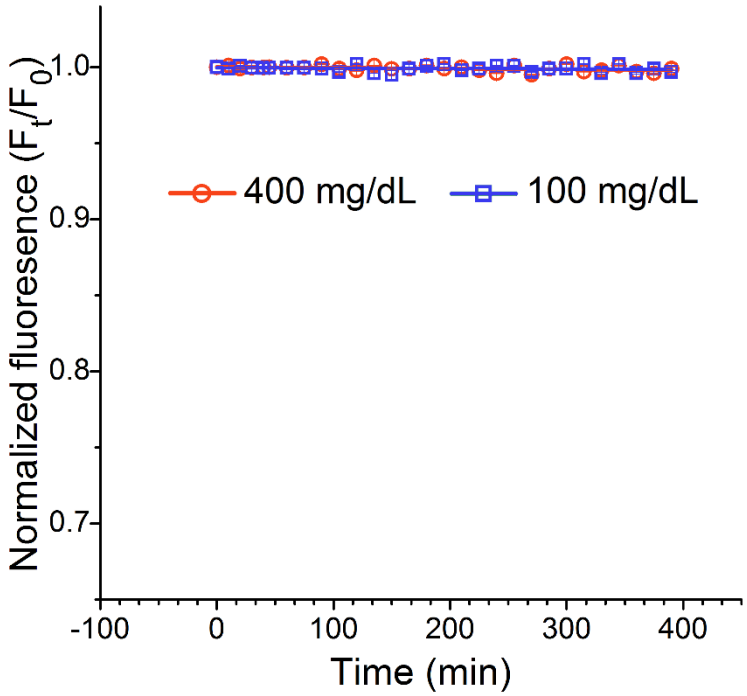

Supplementary Figure 16| FRET assay to study the interactions of the peptide anchored on OLVs and ISVs surfaces at different glucose concentrations, where the ISVs were modified with non-pH-responsive DNA bridged PEG shield, and peptide-K and peptide-E were modified nitrobenzofuran (peptide-donor) and tetramethylrhodamine (peptide-acceptor), respectively. F_0 and F_t represent the fluorescence intensity of peptide-donor measured before and at time t after addition into glucose solutions. The data indicated that by using non-pH-controllable PEG shield, the peptide-K on the ISV surfaces were hindered to interact with the peptide-E on OLV inner surfaces. Data points represent mean ± SD (three independent experiments per group; n=3).

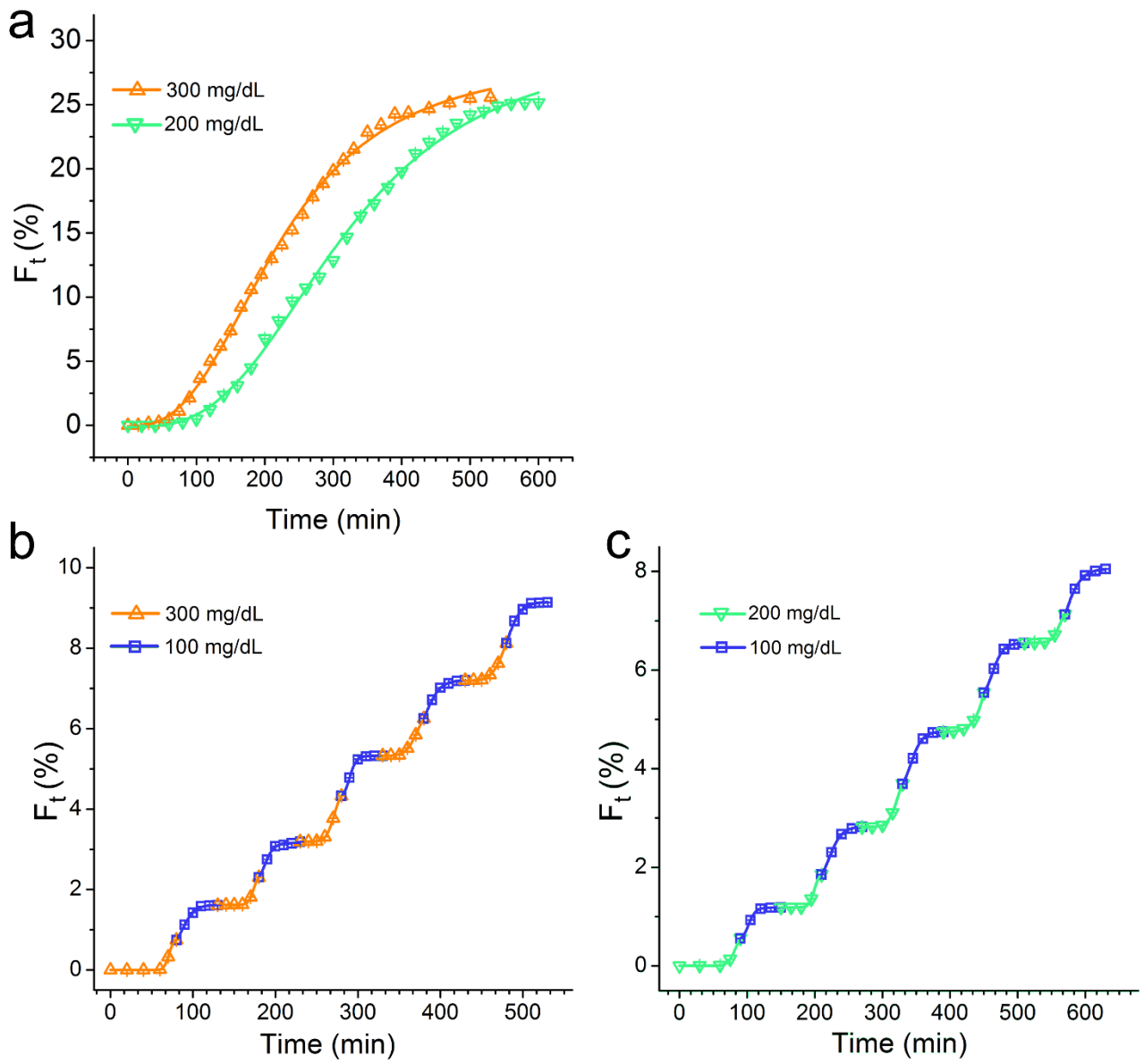

Supplementary Figure 17| a, Kinetics profiles of lipid mixing between lipid-donor/acceptor-labeled ISV and OLV in 300 mg/dL and 200 mg/dl glucose solutions as indicated by the increase in lipid-donor emission. **b** and **c,** Step increase in the fluorescence of lipid-donor after alternatively changing the glucose concentrations. Data points represent mean ± SD (three independent experiments per group; n=3).

Nature Chemical Biology: doi:10.1038/nchembio.2511

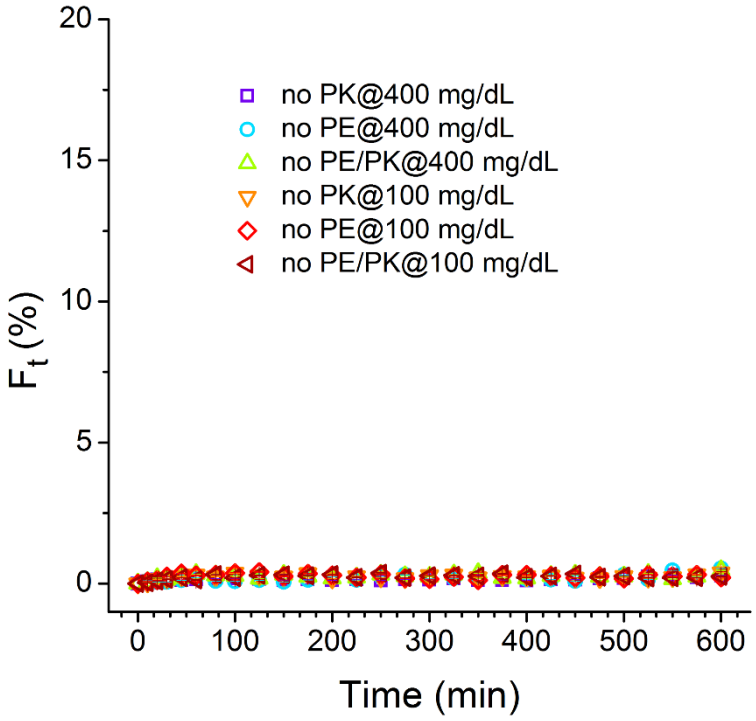

Supplementary Figure 18| Lipid mixing between ISV and OLV as indicated by the variation in NBD florescence in control AβCs in which peptide-K (PK), or peptide-E (PE), or peptide-E and peptide-K (PE/PK) were omitted. It can be seen that lacking the machinery for membrane fusion, no lipid mixing was detected at either high or low glucose concentrations. Data points represent mean ± SD (three independent experiments per group; n=3).

Nature Chemical Biology: doi:10.1038/nchembio.2511

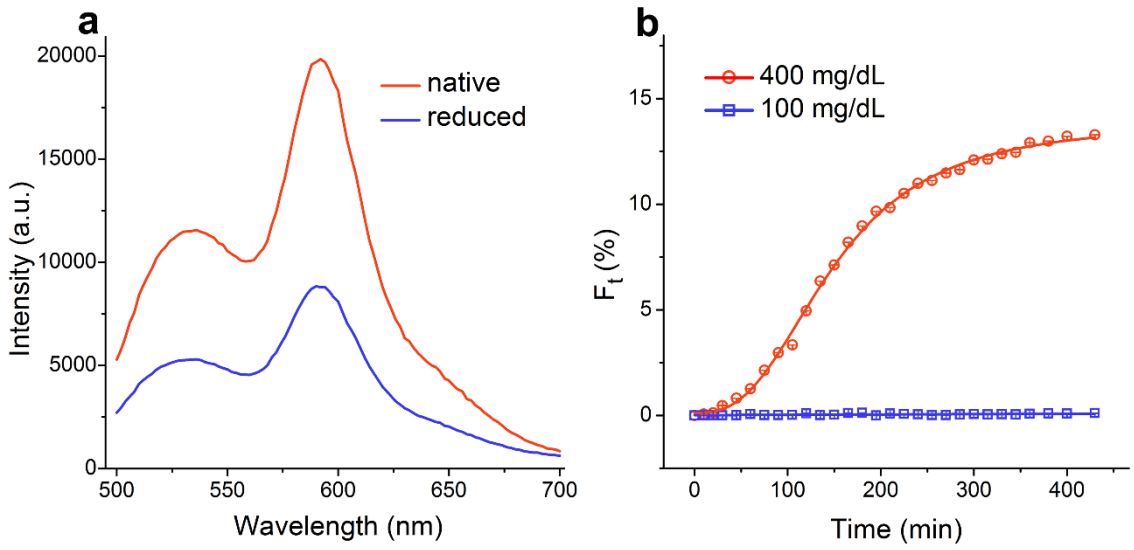

Supplementary Figure 19| a, Fluorescence spectra of lipid-donor/lipid-acceptor co-labeled ISV before (red line) and after (green line) reduction by sodium dithionate. **b,** Kinetics profiles showed the mixing of the inner-layer lipids of lipid-donor/lipid-acceptor co-labeled ISV with OLV in 400 mg/dL and 100 mg/dl glucose solutions as indicated by the increase in lipid-donor emission. Data points represent mean ± SD (three independent experiments per group; n=3).

Nature Chemical Biology: doi:10.1038/nchembio.2511

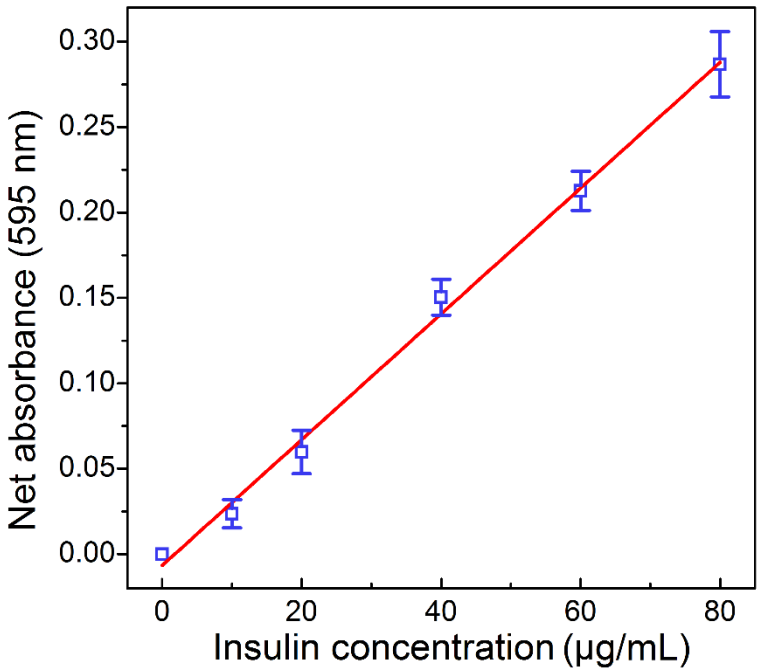

Supplementary Figure 20| Insulin standard curve obtained by Coomassie Plus protein assay. Data points represent mean ± SD (three independent experiments per group; n=3).

Nature Chemical Biology: doi:10.1038/nchembio.2511

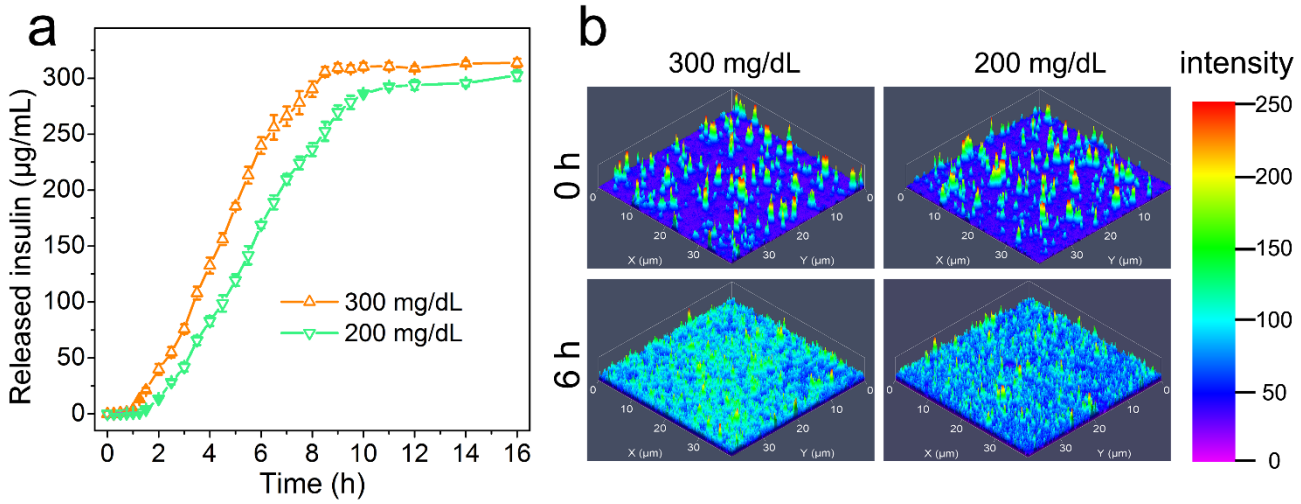

Supplementary Figure 21| a, *In vitro* accumulated insulin release from AβCs incubated in solutions with modest hyperglycemic concentrations. Data points represent mean ± SD (three independent experiments per group; n=3). **b,** 2.5D confocal laser microscopy images showed the fluorescence intensity and distribution of fluorescein labeled-insulin from AβCs before and after incubation in solutions containing different concentrations of glucose.

Nature Chemical Biology: doi:10.1038/nchembio.2511

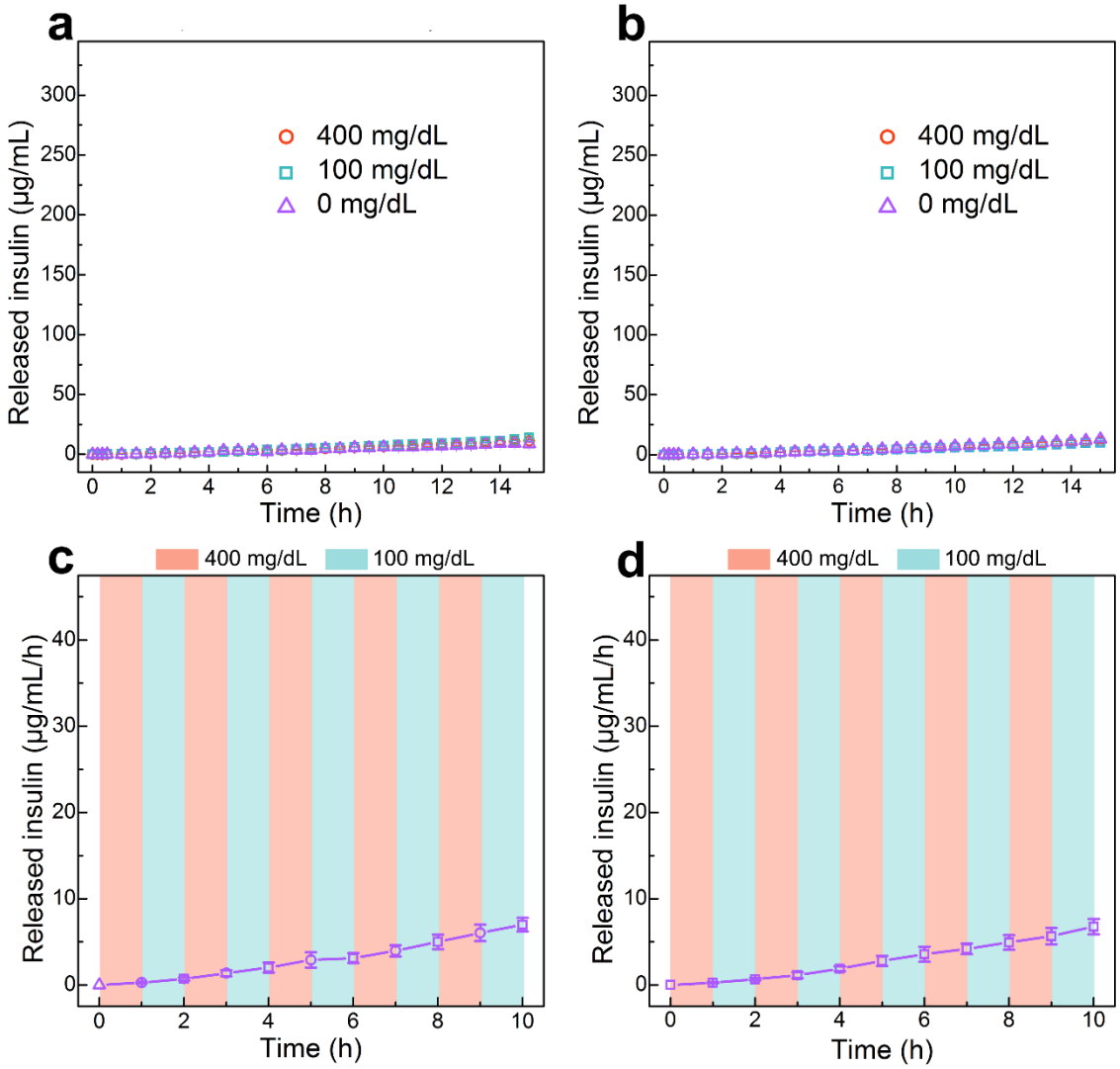

Supplementary Figure 22| *In vitro* accumulated insulin release from control AβCs (**a**) lacking glucose sensing machinery (glucose transporter 2, glucose oxidase/catalase, and gramicidin) and (**b**) with no membrane fusion machinery (peptide-E and peptide-K) at different glucose levels. **c** and **d** respectively showed the rate of the pulsatile insulin release profile by the control AβCs used in **a** and **b** in response to glucose concentration switch between 400 and 100 mg/dL. Data points represent mean ± SD (three independent experiments per group; n=3).

Nature Chemical Biology: doi:10.1038/nchembio.2511

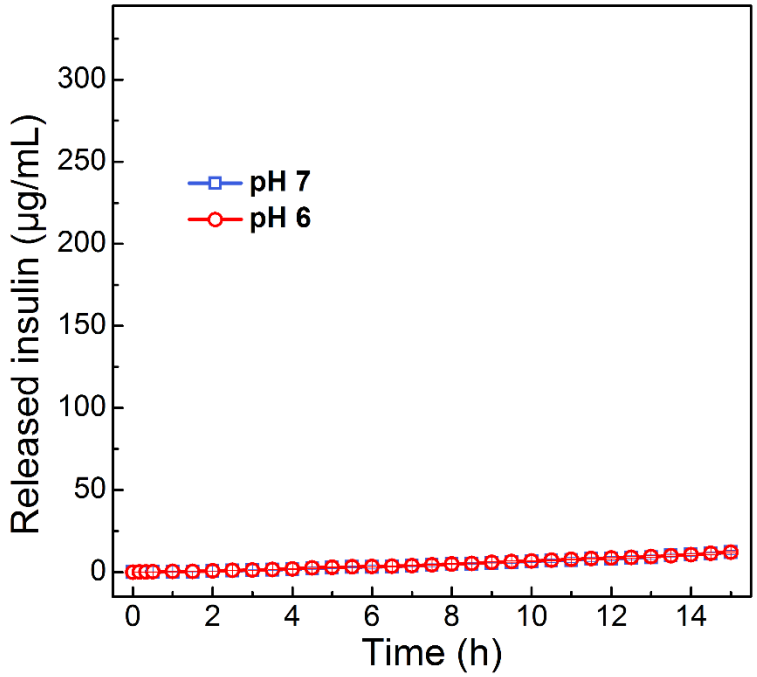

Supplementary Figure 23| *In vitro* accumulated insulin release from AβCs in mild acidic environment. Data points represent mean ± SD (three independent experiments per group; n=3).

Nature Chemical Biology: doi:10.1038/nchembio.2511

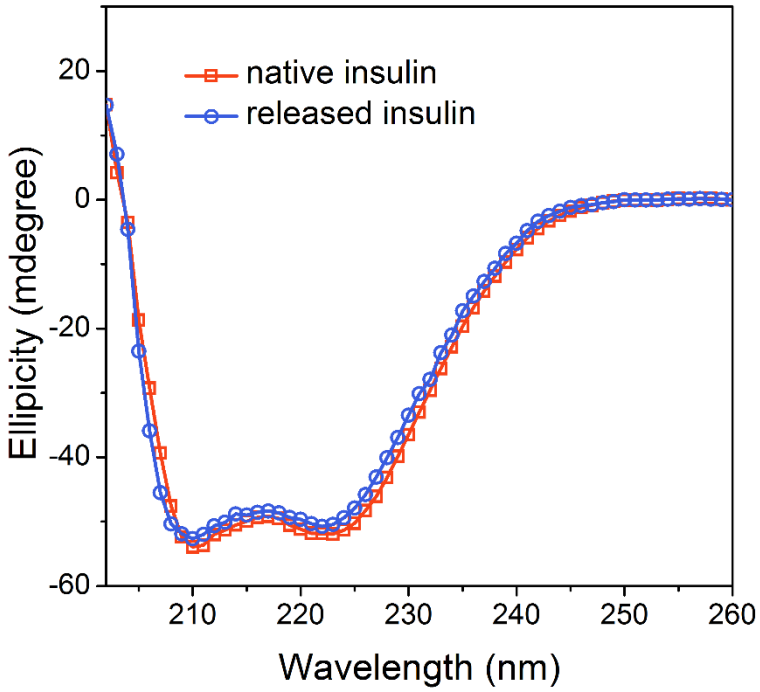

Supplementary Figure 24| CD spectra of the solutions containing native insulins, and released insulins from AβCs incubated with 400 mg/dL glucose. The data indicated that the overall secondary structure of the released insulins was maintained to that of the native insulins.

Nature Chemical Biology: doi:10.1038/nchembio.2511

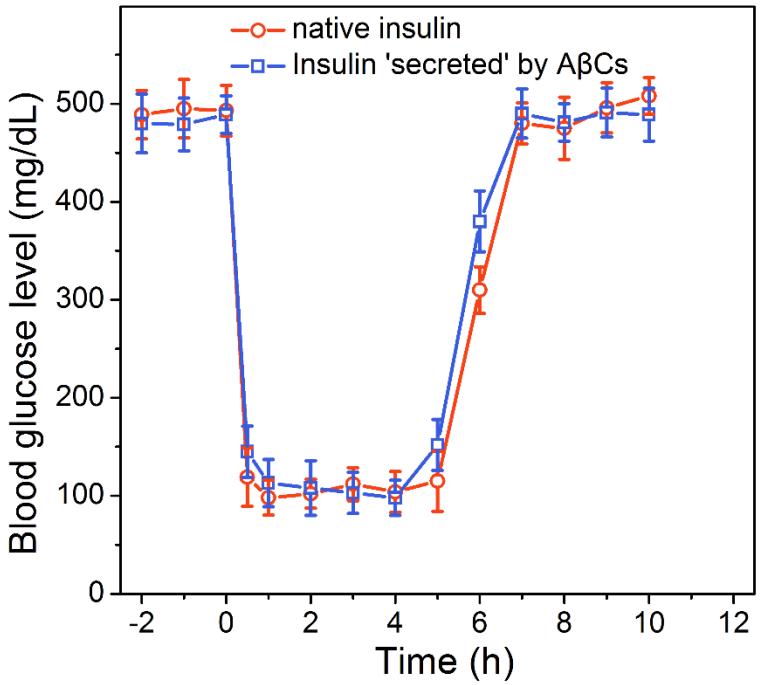

Supplementary Figure 25| Comparison the bioactivity of the insulin 'secreted' by AβCs after incubation with 400 mg/dL glucose and that of native insulin. The results showed that the bioactivity of insulin was highly retained during the AβC preparation and release test. Data points represent mean ± SD (five mice per group; n=5).

Nature Chemical Biology: doi:10.1038/nchembio.2511

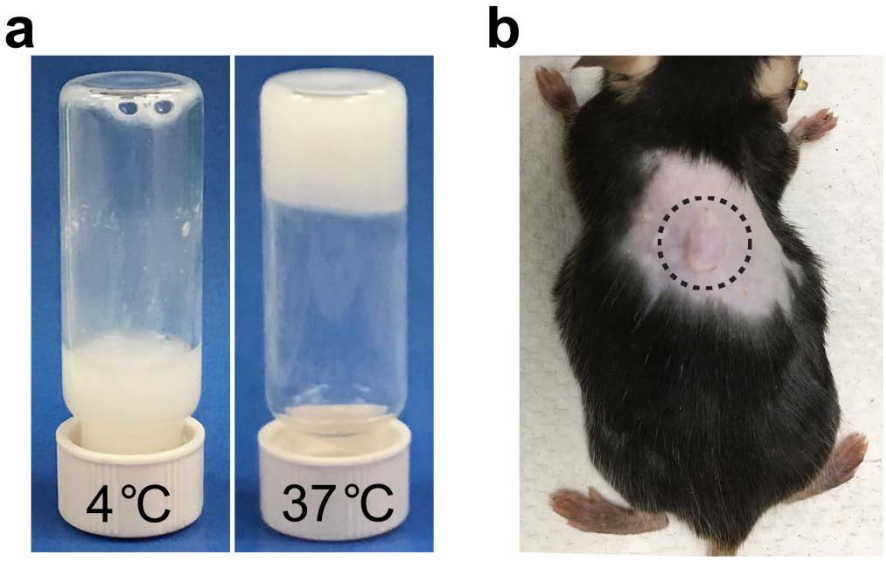

Supplementary Figure 26| AβC integrated thermoresponsive PF127 (40 wt%) solution immediately formed a hydrogel at 37 °C *in vitro* (**a**), and 1 min after subcutaneously injection (**b**). As can be clearly seen in **b**, the hydrogel presented as a 'bump' on the dorsum of the mouse.

Nature Chemical Biology: doi:10.1038/nchembio.2511

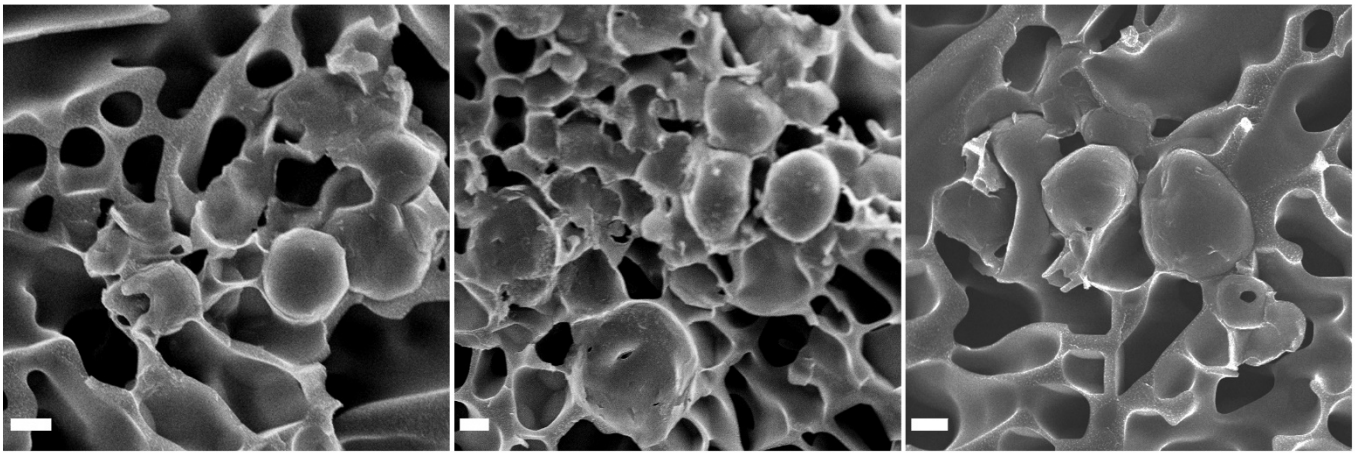

Supplementary Figure 27| Representative cryogenic scanning electron microscopy (cryoSEM) images of the AβC integrated thermoresponsive PF127 solution shown in Supplementary Figure 26. Scale bars: 1 μm.

Nature Chemical Biology: doi:10.1038/nchembio.2511

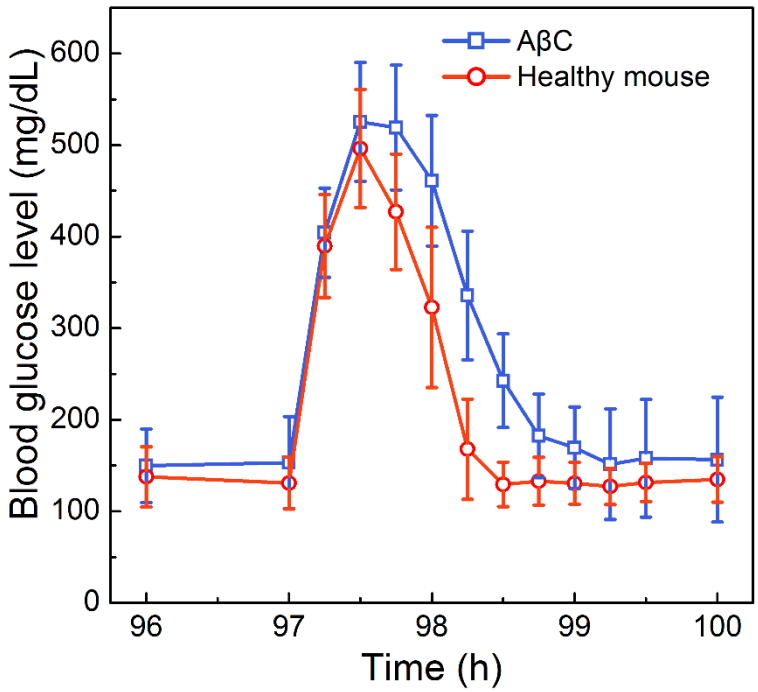

Supplementary Figure 28| *In vivo* intraperitoneal glucose tolerance test (IPGTT) performed toward diabetic mice on day five following A*β*C treatment in comparison to the healthy control mice. Data points represent mean ± SD (five mice per group; n=5).

Nature Chemical Biology: doi:10.1038/nchembio.2511

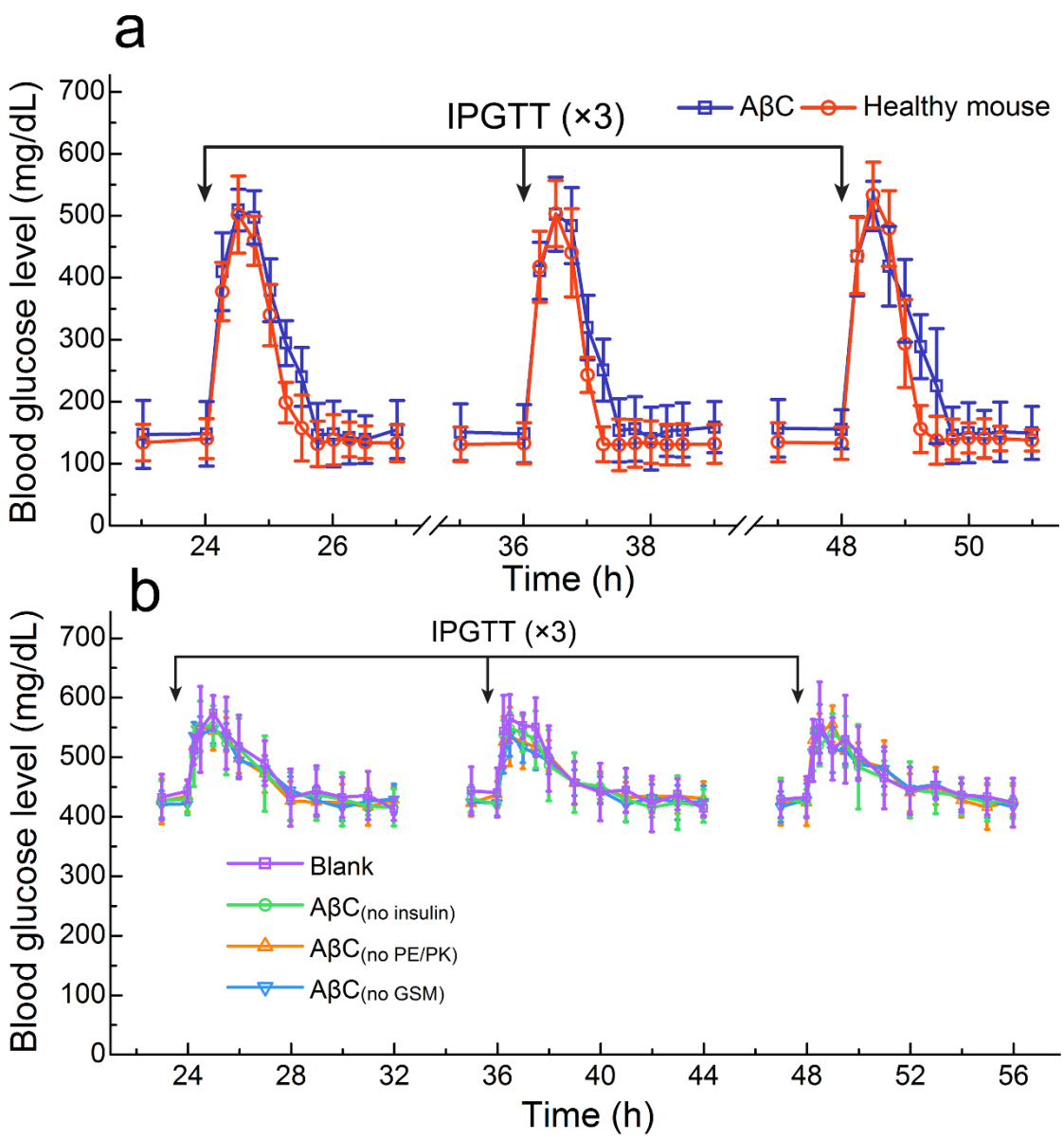

Supplementary Figure 29| (a) *In vivo* intraperitoneal glucose tolerance test (IPGTT) performed toward diabetic mice at 24, 36, and 48 h following AβC treatment in comparison to the healthy control mice. Data points represent mean ± SD (five mice per group; n=5). (b) IPGTT performed toward diabetic mice at 24, 36, and 48 h following treatment with PBS (Blank) and control AβCs. The remained high blood glucose levels in the control groups as well as the insignificant difference in blood glucose variation between PBS-treated and control AβC-treated groups demonstrated the lack of responsiveness of the control AβCs. Data points represent mean ± SD (five mice per group; n=5).

Nature Chemical Biology: doi:10.1038/nchembio.2511

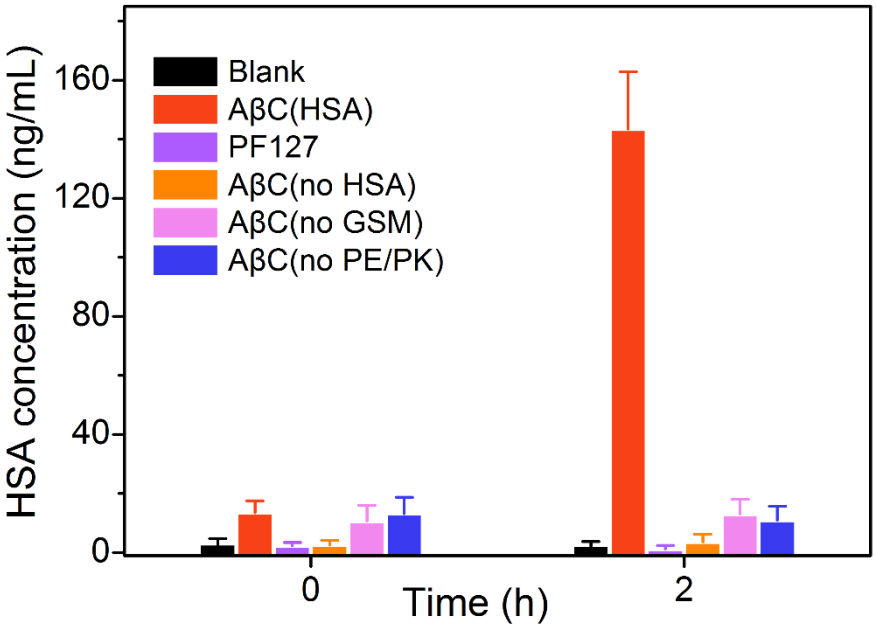

Supplementary Figure 30| *In vivo* intraperitoneal glucose tolerance test (IPGTT) performed towards wild-type mice transplanted with A*β*Cs that were loaded with human serum albumin (HSA) as a reporter protein. The human serum albumin in the serum of each group were measured by ELISA at 2 h after intraperitoneal injection of 50 mg glucose/mouse. Data points represent mean ± SD (five mice per group; n=5).

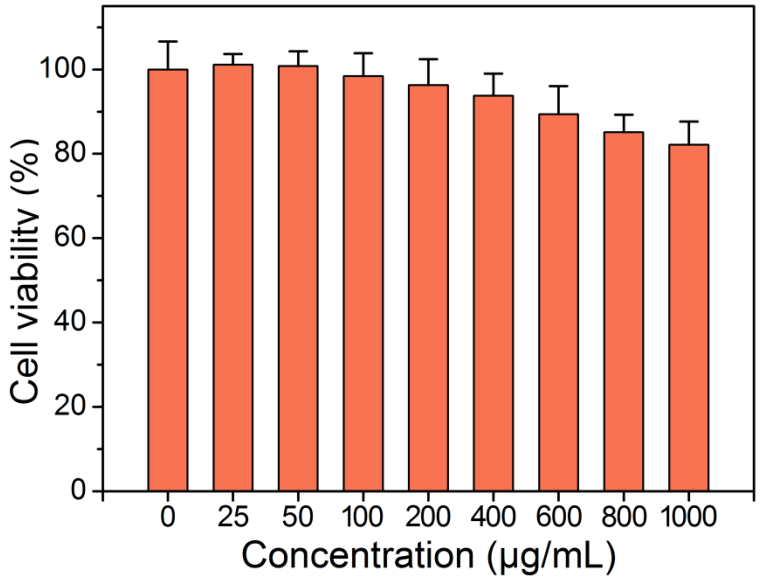

Supplementary Figure 31| Cytotoxicity assay of insulin-free AβC toward HeLa cells after 24 h incubation. Data points represent mean ± SD (three independent experiments per group; n=3).

Nature Chemical Biology: doi:10.1038/nchembio.2511

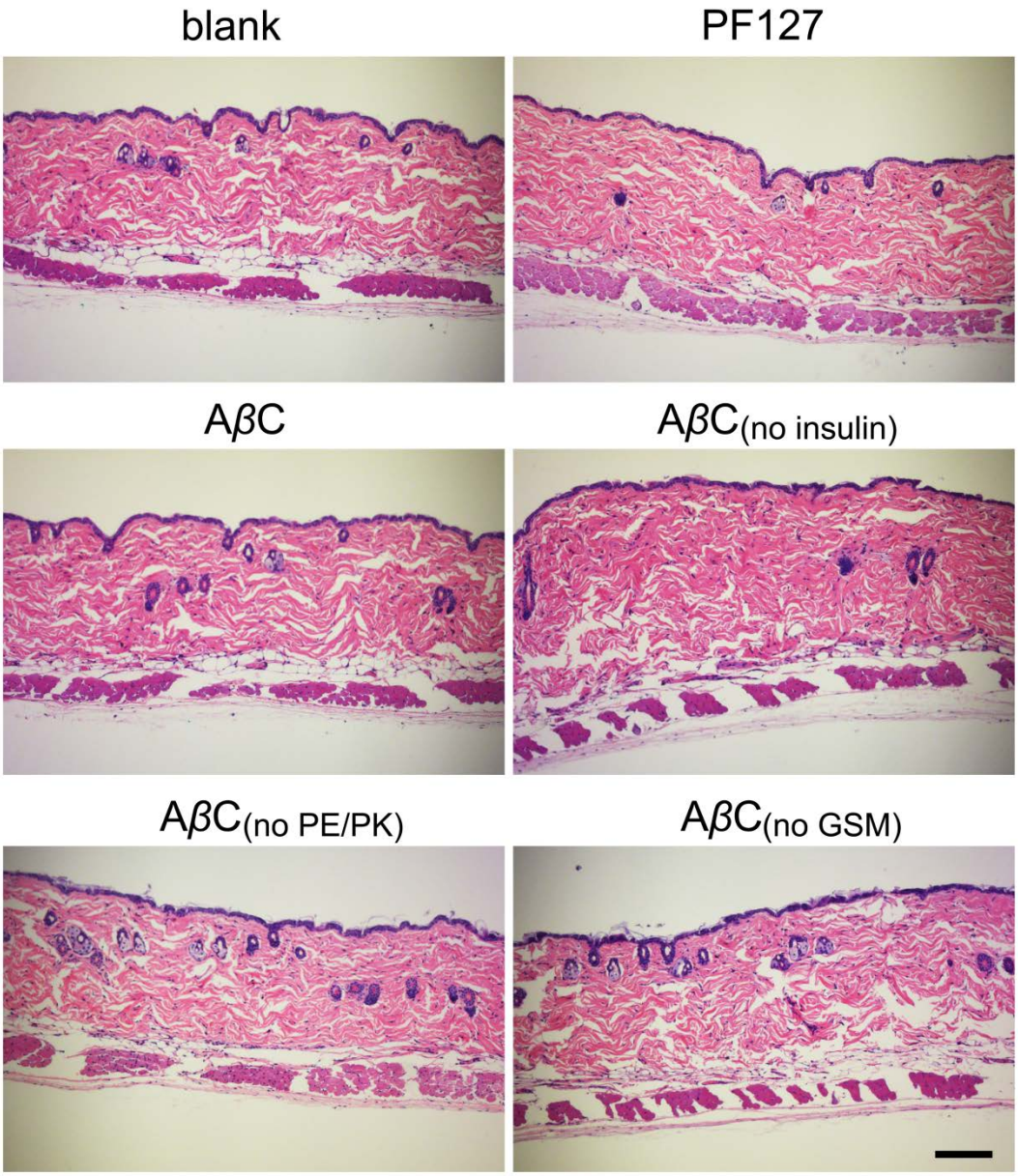

Supplementary Figure 32| Hematoxylin and eosin-stained sections of subcutaneously injected with PBS solution (blank), PF127 thermogel, or 'transplanted' with AβC, AβC$_{(no\ insulin)}$, AβC$_{(no\ PE/PK)}$, or AβC$_{(no\ GSM)}$ after four weeks, respectively. From the graph it can be seen that all the components were degraded and no noticeable inflammatory region or fibrotic encapsulation was observed, indicating the biocompatibility of the artificial assemblies. Scale bar: 150 μm.

Nature Chemical Biology: doi:10.1038/nchembio.2511

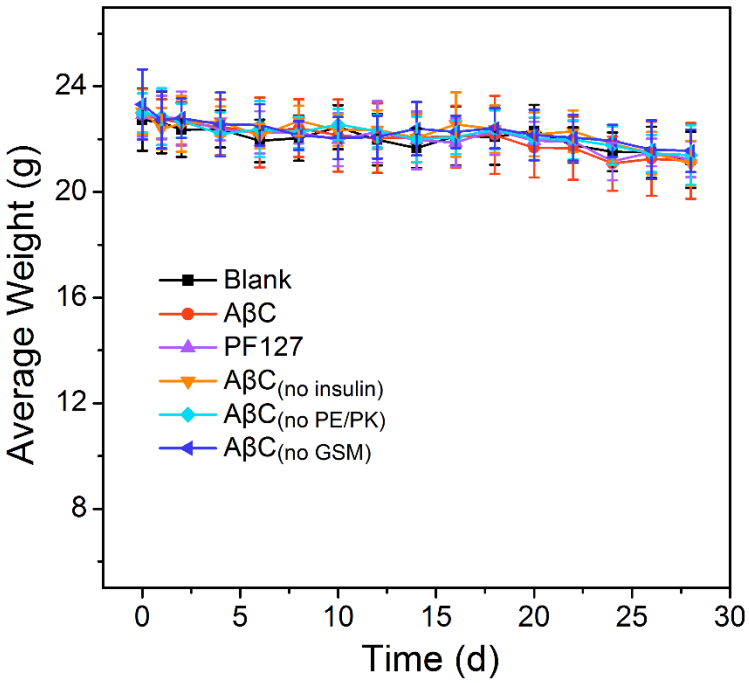

Supplementary Figure 33| Average body weight of the diabetes mice after injection with PBS solution (blank), PF127 thermogel, or 'transplanted' with AβC, AβC$_{(\text{no insulin})}$, AβC$_{(\text{no PE/PK})}$, or AβC$_{(\text{no GSM})}$ for four weeks, respectively. Data points represent mean ± SD (five mice per group; n=5).

Nature Chemical Biology: doi:10.1038/nchembio.2511

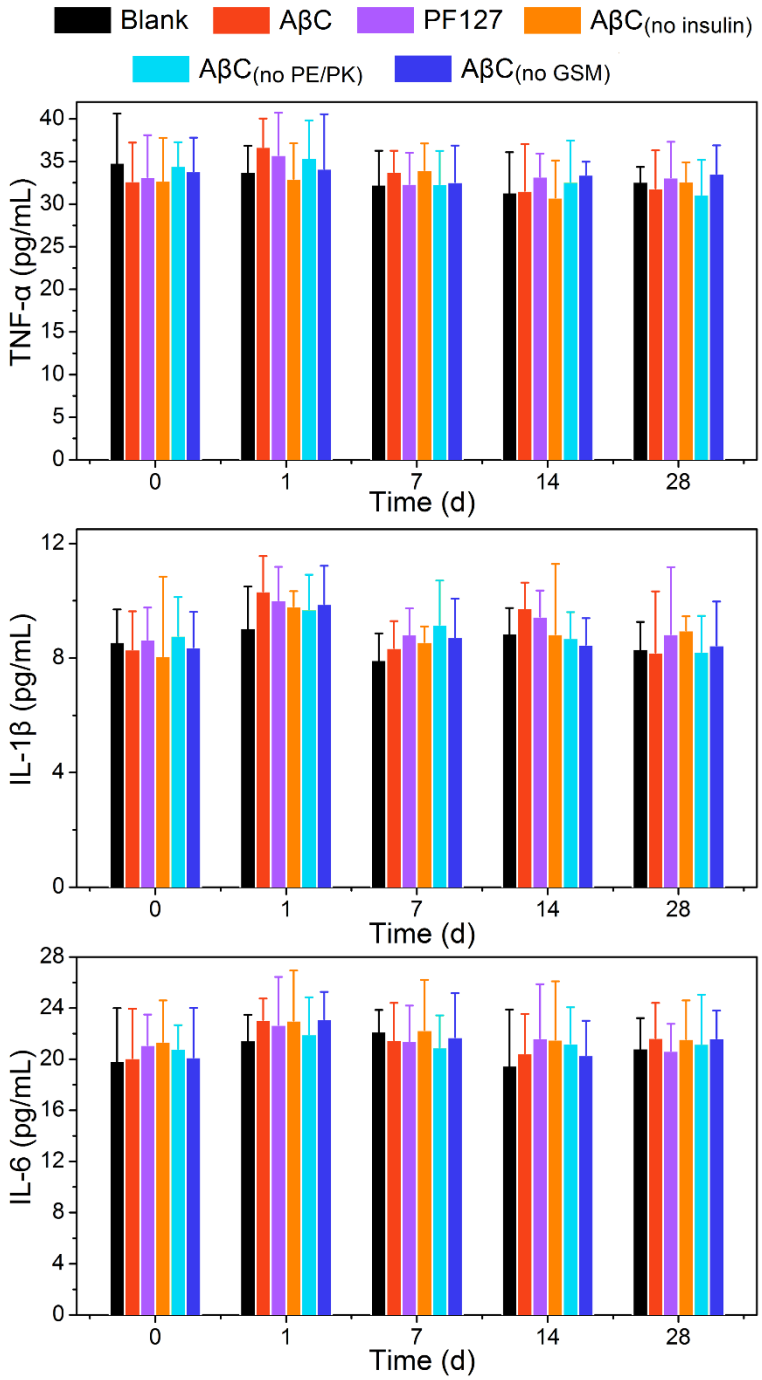

Supplementary Figure 34| Serum levels of TNF-α, IL-1β and IL-6 in diabetes mice after injection with PBS solution (blank), PF127 thermogel, or 'transplanted' with AβC, AβC$_{(no\ insulin)}$, AβC$_{(no\ PE/PK)}$, or AβC$_{(no\ GSM)}$, respectively. Data points represent mean ± SD (five mice per group; n=5).

Nature Chemical Biology: doi:10.1038/nchembio.2511

Supplementary Table:

Supplementary Table 1. The DNA sequences used for synthesis of PEG shield.

pH-responsive DNA	CDNA	5'-CCC TTA CCC TTA CCC TTA CCC TTT TTT-SH-3'
	TAMRA-labeled CDNA	5'-CCC TAA CCC TAA CCC TAA CCC T/i5-TAMK/T TTT T-SH-3'
	*GDNA	5'-GGG TTA GGG TTA GGG TTA GGG TTT TTT-CH-3'
	IAbRQ-labeled GDNA	5'-IAbRQ-GGG TTA GGG TTA GGG TTA GGG TTT TTT-CH-3'
Non-pH-responsive DNA	DNA1	5'-CTC TCA CAC TCA CTC TCA CGC TTT TTT-SH-3'
	TAMRA-labeled DNA1	5'-CTC TCA CAC TCA CTC TCA CGC T/i5-TAMK/TT TTT-SH-3'
	DNA2	5'-GCG TGA GAG TGA GTG TGA GAG TTT TTT-CH-3'
	IAbRQ-labeled DNA2	5'-IAbRQ-GCG TGA GAG TGA GTG TGA GAG TTT TTT-CH-3'

*The three mismatch bases at the partial complementary region of CDNA and GDNA could accelerate the conformational transition process at mildly acidic pH.[39]

Supplementary Movie 1| A movie showing the liposomes-in-liposome superstructures. The inner small liposomes were incorporated with lipids labelled with nitrobenzofuran and outer larger liposome was incorporated with lipids labeled with lissamine rhodamine B. It can be seen that the small particles were moving randomly by Brownian motion inside the large liposomes.

Supplementary Note 1| Plasmid map and full plasmid sequence for glucose transporter 2 (GLUT2).

Nature Chemical Biology: doi:10.1038/nchembio.2511

Supplementary Note 1| Plasmid map and full plasmid sequence for glucose transporter 2 (GLUT2). GLUT2 sequence is highlighted in red and pET28a plasmid backbone sequence in black.

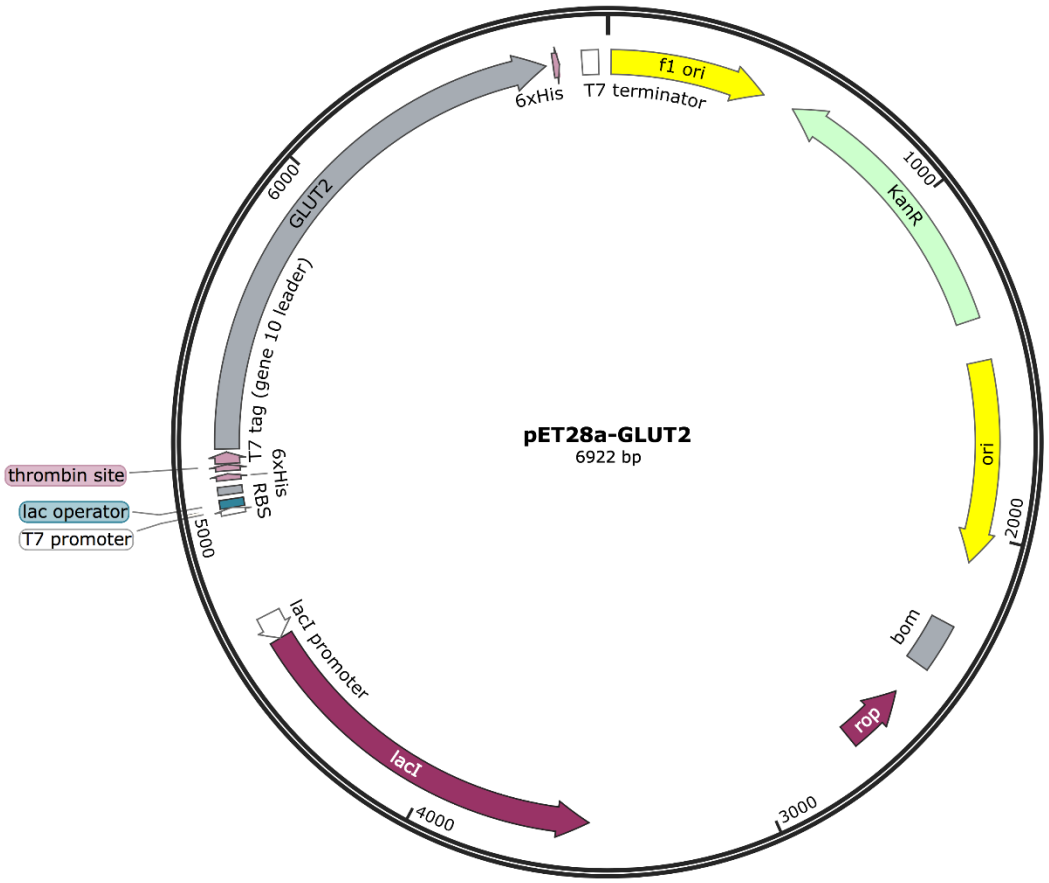

TGGCGAATGGGACGCGCCCTGTAGCGGCGCATTAAGCGCGGCGGGTGTGGTGGTT
ACGCGCAGCGTGACCGCTACACTTGCCAGCGCCCTAGCGCCCGCTCCTTTCGCTTT
CTTCCCTTCCTTTCTCGCCACGTTCGCCGGCTTTCCCCGTCAAGCTCTAAATCGGG
GGCTCCCTTTAGGGTTCCGATTTAGTGCTTTACGGCACCTCGACCCCAAAAAACTT
GATTAGGGTGATGGTTCACGTAGTGGGCCATCGCCCTGATAGACGGTTTTTCGCCC
TTTGACGTTGGAGTCCACGTTCTTTAATAGTGGACTCTTGTTCCAAACTGGAACAA
CACTCAACCCTATCTCGGTCTATTCTTTTGATTTATAAGGGATTTTGCCGATTTCGGC
CTATTGGTTAAAAAATGAGCTGATTTAACAAAAATTTAACGCGAATTTTAACAAAAT
ATTAACGTTTACAATTTCAGGTGGCACTTTTCGGGGAAATGTGCGCGGAACCCCTA
TTTGTTTATTTTTCTAAATACATTCAAATATGTATCCGCTCATGAATTAATTCTTAGAA
AAACTCATCGAGCATCAAATGAAACTGCAATTTATTCATATCAGGATTATCAATACC
ATATTTTTGAAAAAGCCGTTTCTGTAATGAAGGAGAAAACTCACCGAGGCAGTTCC
ATAGGATGGCAAGATCCTGGTATCGGTCTGCGATTCCGACTCGTCCAACATCAATA
CAACCTATTAATTTCCCCTCGTCAAAAATAAGGTTATCAAGTGAGAAATCACCATG

AGTGACGACTGAATCCGGTGAGAATGGCAAAAGTTTATGCATTTCTTTCCAGACTT
GTTCAACAGGCCAGCCATTACGCTCGTCATCAAAATCACTCGCATCAACCAAACCG
TTATTCATTCGTGATTGCGCCTGAGCGAGACGAAATACGCGATCGCTGTTAAAAGG
ACAATTACAAACAGGAATCGAATGCAACCGGCGCAGGAACACTGCCAGCGCATCA
ACAATATTTTCACCTGAATCAGGATATTCTTCTAATACCTGGAATGCTGTTTTCCCGG
GGATCGCAGTGGTGAGTAACCATGCATCATCAGGAGTACGGATAAAATGCTTGATG
GTCGGAAGAGGCATAAATTCCGTCAGCCAGTTTAGTCTGACCATCTCATCTGTAAC
ATCATTGGCAACGCTACCTTTGCCATGTTTCAGAAACAACTCTGGCGCATCGGGCT
TCCCATACAATCGATAGATTGTCGCACCTGATTGCCCGACATTATCGCGAGCCCATT
TATACCCATATAAATCAGCATCCATGTTGGAATTTAATCGCGGCCTAGAGCAAGACG
TTTCCCGTTGAATATGGCTCATAACACCCCTTGTATTACTGTTTATGTAAGCAGACA
GTTTTATTGTTCATGACCAAAATCCCTTAACGTGAGTTTTCGTTCCACTGAGCGTCA
GACCCCGTAGAAAAGATCAAAGGATCTTCTTGAGATCCTTTTTTTCTGCGCGTAAT
CTGCTGCTTGCAAACAAAAAAACCACCGCTACCAGCGGTGGTTTGTTTGCCGGAT
CAAGAGCTACCAACTCTTTTTCCGAAGGTAACTGGCTTCAGCAGAGCGCAGATAC
CAAATACTGTCCTTCTAGTGTAGCCGTAGTTAGGCCACCACTTCAAGAACTCTGTA
GCACCGCCTACATACCTCGCTCTGCTAATCCTGTTACCAGTGGCTGCTGCCAGTGG
CGATAAGTCGTGTCTTACCGGGTTGGACTCAAGACGATAGTTACCGGATAAGGCGC
AGCGGTCGGGCTGAACGGGGGGTTCGTGCACACAGCCCAGCTTGGAGCGAACGA
CCTACACCGAACTGAGATACCTACAGCGTGAGCTATGAGAAAGCGCCACGCTTCC
CGAAGGGAGAAAGGCGGACAGGTATCCGGTAAGCGGCAGGGTCGGAACAGGAG
AGCGCACGAGGGAGCTTCCAGGGGGAAACGCCTGGTATCTTTATAGTCCTGTCGG
GTTTCGCCACCTCTGACTTGAGCGTCGATTTTTGTGATGCTCGTCAGGGGGGCGGA
GCCTATGGAAAAACGCCAGCAACGCGGCCTTTTTACGGTTCCTGGCCTTTTGCTGG
CCTTTTGCTCACATGTTCTTTCCTGCGTTATCCCCTGATTCTGTGGATAACCGTATTA
CCGCCTTTGAGTGAGCTGATACCGCTCGCCGCAGCCGAACGACCGAGCGCAGCGA
GTCAGTGAGCGAGGAAGCGGAAGAGCGCCTGATGCGGTATTTTCTCCTTACGCAT
CTGTGCGGTATTTCACACCGCATATATGGTGCACTCTCAGTACAATCTGCTCTGATG
CCGCATAGTTAAGCCAGTATACACTCCGCTATCGCTACGTGACTGGGTCATGGCTGC
GCCCCGACACCCGCCAACACCCGCTGACGCGCCCTGACGGGCTTGTCTGCTCCCG
GCATCCGCTTACAGACAAGCTGTGACCGTCTCCGGGAGCTGCATGTGTCAGAGGT
TTTCACCGTCATCACCGAAACGCGCGAGGCAGCTGCGGTAAAGCTCATCAGCGTG
GTCGTGAAGCGATTCACAGATGTCTGCCTGTTCATCCGCGTCCAGCTCGTTGAGTT
TCTCCAGAAGCGTTAATGTCTGGCTTCTGATAAAGCGGGCCATGTTAAGGGCGGTT
TTTTCCTGTTTGGTCACTGATGCCTCCGTGTAAGGGGGATTTCTGTTCATGGGGGTA
ATGATACCGATGAAACGAGAGAGGATGCTCACGATACGGGTTACTGATGATGAACA
TGCCCGGTTACTGGAACGTTGTGAGGGTAAACAACTGGCGGTATGGATGCGGCGG
GACCAGAGAAAAATCACTCAGGGTCAATGCCAGCGCTTCGTTAATACAGATGTAG
GTGTTCCACAGGGTAGCCAGCAGCATCCTGCGATGCAGATCCGGAACATAATGGTG
CAGGGCGCTGACTTCCGCGTTTCCAGACTTTACGAAACACGGAAACCGAAGACCA
TTCATGTTGTTGCTCAGGTCGCAGACGTTTTGCAGCAGCAGTCGCTTCACGTTCGC
TCGCGTATCGGTGATTCATTCTGCTAACCAGTAAGGCAACCCCGCCAGCCTAGCCG
GGTCCTCAACGACAGGAGCACGATCATGCGCACCCGTGGGGCCGCCATGCCGGCG
ATAATGGCCTGCTTCTCGCCGAAACGTTTGGTGGCGGGACCAGTGACGAAGGCTT

GAGCGAGGGCGTGCAAGATTCCGAATACCGCAAGCGACAGGCCGATCATCGTCGC
GCTCCAGCGAAAGCGGTCCTCGCCGAAAATGACCCAGAGCGCTGCCGGCACCTGT
CCTACGAGTTGCATGATAAAGAAGACAGTCATAAGTGCGGCGACGATAGTCATGCC
CCGCGCCCACCGGAAGGAGCTGACTGGGTTGAAGGCTCTCAAGGGCATCGGTCG
AGATCCCGGTGCCTAATGAGTGAGCTAACTTACATTAATTGCGTTGCGCTCACTGC
CCGCTTTCCAGTCGGGAAACCTGTCGTGCCAGCTGCATTAATGAATCGGCCAACGC
GCGGGGAGAGGCGGTTTGCGTATTGGGCGCCAGGGTGGTTTTTCTTTTCACCAGT
GAGACGGGCAACAGCTGATTGCCCTTCACCGCCTGGCCCTGAGAGAGTTGCAGCA
AGCGGTCCACGCTGGTTTGCCCCAGCAGGCGAAAATCCTGTTTGATGGTGGTTAA
CGGCGGGATATAACATGAGCTGTCTTCGGTATCGTCGTATCCCACTACCGAGATATC
CGCACCAACGCGCAGCCCGGACTCGGTAATGGCGCGCATTGCGCCCAGCGCCATC
TGATCGTTGGCAACCAGCATCGCAGTGGGAACGATGCCCTCATTCAGCATTTGCAT
GGTTTGTTGAAAACCGGACATGGCACTCCAGTCGCCTTCCCGTTCCGCTATCGGCT
GAATTTGATTGCGAGTGAGATATTTATGCCAGCCAGCCAGACGCAGACGCGCCGA
GACAGAACTTAATGGGCCCGCTAACAGCGCGATTTGCTGGTGACCCAATGCGACC
AGATGCTCCACGCCCAGTCGCGTACCGTCTTCATGGGAGAAAATAATACTGTTGAT
GGGTGTCTGGTCAGAGACATCAAGAAATAACGCCGGAACATTAGTGCAGGCAGCT
TCCACAGCAATGGCATCCTGGTCATCCAGCGGATAGTTAATGATCAGCCCACTGAC
GCGTTGCGCGAGAAGATTGTGCACCGCCGCTTTACAGGCTTCGACGCCGCTTCGTT
CTACCATCGACACCACCACGCTGGCACCCAGTTGATCGGCGCGAGATTTAATCGCC
GCGACAATTTGCGACGGCGCGTGCAGGGCCAGACTGGAGGTGGCAACGCCAATC
AGCAACGACTGTTTGCCCGCCAGTTGTTGTGCCACGCGGTTGGGAATGTAATTCAG
CTCCGCCATCGCCGCTTCCACTTTTTCCCGCGTTTTCGCAGAAACGTGGCTGGCCT
GGTTCACCACGCGGGAAACGGTCTGATAAGAGACACCGGCATACTCTGCGACATC
GTATAACGTTACTGGTTTCACATTCACCACCCTGAATTGACTCTCTTCCGGGCGCTA
TCATGCCATACCGCGAAAGGTTTTGCGCCATTCGATGGTGTCCGGGATCTCGACGC
TCTCCCTTATGCGACTCCTGCATTAGGAAGCAGCCCAGTAGTAGGTTGAGGCCGTT
GAGCACCGCCGCCGCAAGGAATGGTGCATGCAAGGAGATGGCGCCCAACAGTCC
CCCGGCCACGGGGCCTGCCACCATACCCACGCCGAAACAAGCGCTCATGAGCCCG
AAGTGGCGAGCCCGATCTTCCCCATCGGTGATGTCGGCGATATAGGCGCCAGCAAC
CGCACCTGTGGCGCCGGTGATGCCGGCCACGATGCGTCCGGCGTAGAGGATCGAG
ATCTCGATCCCGCGAAATTAATACGACTCACTATAGGGGAATTGTGAGCGGATAAC
AATTCCCCTCTAGAAATAATTTTGTTTAACTTTAAGAAGGAGATATACCATGGGCAG
CAGCCATCATCATCATCATCACAGCAGCGGCCTGGTGCCGCGCGGCAGCCATATGG
CTAGCATGACTGGTGGACAGCAAATGGGTCGCGGATCCATGTCAGAAGACAAGAT
CACCGGAACCTTGGCTTTCACTGTCTTCACTGCTGTACTGAGTTCCTTCCAGTTCG
GCTATGACATCGGTGTGATCAATGCACCTCAAGAGGTAATAATATCCCATTATCGAC
ATGTTTTGGGTGTTCCACTGGATGACCGGAAAGCTGCCATTAACTATGACGTCAAT
GGCACAGACACCCCACTTACAGTCACACCAGCATACACAACACCAGCTCCCTGGG
ATGAAGAGGAGACTGAAGGATCTGCTCACATAGTCACTATGCTCTGGTCTCTGTCT
GTGTCCAGCTTTGCAGTGGGCGGAATGGTCGCCTCATTCTTTGGTGGGTGGCTCGG
GGACAAACTTGGAAGGATCAAAGCAATGTTGGCTGCAAACAGCCTCTCATTGACT
GGAGCCCTCTTGATGGGATGTTCCAAATTTGGACCGGCACACGCCCTCATCATTGC
TGGACGAAGTGTATCAGGACTGTATTGTGGGCTAATTTCAGGACTGGTTCCAATGT

ACATTGGAGAGATCGCTCCAACCACACTCAGGGGTGCCCTGGGTACTCTTCACCA
ACTGGCCCTTGTCACAGGCATTCTTATTAGTCAGATTGCTGGCCTCAGCTTTATTCT
GGGCAATCAGGATCATTGGCACATCCTACTTGGCCTATCTGCTGTGCCAGCTCTTCT
GCAGTGTCTGCTACTGCTCTTCTGTCCAGAAAGCCCCAGATACCTTTATATAAAGTT
GGAAGAGGAAGTCAGGGCAAAGAAAAGCTTGAAGAGACTAAGAGGAACTGAGG
ATGTCACCAAAGATATTAATGAGATGAAGAAAGAAAAGGAAGAGGCATCGACTGA
GCAGAAGGTCTCCGTGATCCAGCTCTTCACGGATGCCAATTACCGACAGCCCATCC
TCGTGGCGCTGATGCTGCACATGGCCCAGCAGTTCTCAGGAATCAATGGGATATTT
TACTATTCAACCAGCATTTTTCAGACAGCTGGCATCAGCCAGCCTGTGTATGCAAC
CATTGGTGTTGGGGCCATCAACATGATCTTCACGGCTGTCTCTGTGCTGCTTGTGG
AGAAGGCAGGGCGGCGGACCCTGTTCCTAACCGGGATGATTGGCATGTTTTTCTGC
ACCATCTTCATGTCGGTGGGACTTGTGCTGCTGGATAAATTCGCCTGGATGAGTTA
CGTGAGCATGACTGCCATCTTCCTCTTTGTCAGTTTCTTTGAGATTGGGCCAGGTC
CAATCCCTTGGTTCATGGTTGCTGAATTTTTCAGCCAAGGACCCCGTCCTACGGCT
CTGGCACTGGCTGCCTTCAGCAACTGGGTCTGCAATTTTGTCATCGCCCTCTGCTT
CCAGTACATTGCGGACTTCCTTGGGCCTTACGTGTTCTTCCTCTTCGCTGGGGTGG
TCCTGGTCTTCACCCTGTTTACATTCTTTAAAGTTCCAGAAACCAAAGGAAAGTCT
TTTGAGGAAATCGCTGCAGAATTCCGGAAGAAGAGTGGTTCGGCCCCACCACGCA
AAGCTGCTGTACAAATGGAATTCCTGGCGTCTTCAGAGAGTGTGTGAAAGCTTGC
GGCCGCACTCGAGCACCACCACCACCACCACTGAGATCCGGCTGCTAACAAAGCC
CGAAAGGAAGCTGAGTTGGCTGCTGCCACCGCTGAGCAATAACTAGCATAACCCC
TTGGGGCCTCTAAACGGGTCTTGAGGGGTTTTTTGCTGAAAGGAGGAACTATATCC
GGAT